Environmental Science Nano

ROYAL SOCIETY OF CHEMISTRY

CRITICAL REVIEW

View Article Online
View Journal

Check for updates

Cite this: DOI: 10.1039/d5en00630a

A physical chemistry lens on environmental nanoplastics analysis challenges. Part II: detection techniques – principles, limitations and future directions

Manpreet Kaur,[a] Christopher T. Gibson,[b] Sara J. Fraser-Miller,[a] Sophie C. Leterme [a] and Melanie Macgregor *[a]

Nanoplastics (NPs) have become a prominent environmental pollutant, garnering increasing scientific and public attention due to their possible effects on ecosystems and human health. However, their detection remains a major analytical challenge due to their small size, diverse polymeric compositions, and unique surface properties facilitating strong interactions with complex environmental matrices. To date, no single technique can provide complete information on their identity, morphology, and concentration, and many existing methods fail when adapted from microplastics workflows. This review aims to provide a comparative evaluation of current detection approaches for NPs, with a special focus on the physical principles underpinning each technique and how these principles affect their performance at the nanoscale. Spectroscopic (*e.g.* FTIR, Raman, XPS), mass-based (*e.g.* pyrolysis-GC-MS, MALDI-TOF), imaging (*e.g.* SEM, TEM, fluorescence microscopy), and population-level (*e.g.* DLS, NTA, flow cytometry) methods are discussed in terms of what they measure, how they work, and why their applicability to NPs may be limited. Rather than presenting techniques as black boxes, this review explains their working principle in the context of NPs research needs, offering a tangible way to understand what each method can—and cannot—reveal about NPs in terms of polymer classification and surface chemistry, quantification, morphological analysis, size distribution, and concentration. The merits and drawbacks of each technique are assessed, emphasizing their complementary roles in addressing the challenges of NP analysis. The originality of this review lies in its principle-based evaluation of detection methods, a comparative synthesis table that informs multimodal workflows, and a standards-oriented roadmap. This roadmap connects the current MP framework to the future requirements of NP research—harmonised methods, cross-laboratory comparability, and reliable data to underpin future monitoring and remediation efforts.

Received 11th July 2025,
Accepted 20th October 2025

DOI: 10.1039/d5en00630a

rsc.li/es-nano

Published on 30 2025. Downloaded on 25.5.2026 16:41:33.

Environmental significance

Nanoplastics (NPs) remain difficult to characterise due to their small size, low signal strength, and complex composition. This review critically examines current detection and characterisation techniques, highlighting how underlying physical principles constrain their performance. By clarifying the analytical limits and suitability of each method, it supports the development of reliable workflows essential for environmental monitoring and regulatory decision-making on NPs.

1 Introduction

Nanoplastics (NPs) are an emerging class of environmental pollutants that pose unique analytical challenges due to their small size, distinct physico-chemical properties, and high potential for biological interactions. Defined as plastic particles smaller than one micrometer, NPs are significantly more difficult to study than microplastics (MPs) due to their nanoscale dimensions and complex interactions with surrounding environmental matrices. Yet their presence in terrestrial and marine ecosystems is expected to be just as widespread[1] and their potential toxicity is increasingly recognised—with reports demonstrating NPs affecting organisms from the base to the top of the food chain.[2–4]

[a] College of Science and Engineering, Flinders University, Bedford Park 5048, Australia. E-mail: melanie.macgregor@flinders.edu.au
[b] Adelaide Microscopy, The University of Adelaide, Adelaide 5005, Australia

Published on 30 2025. Downloaded on 25.5.2026 16:41:33.

Suitable analytical techniques tailored to NPs are essential to addressing a critical gap in our understanding of their environmental prevalence, fate, and potential toxicity.

In part 1 of this review, we explored the fundamental differences between NPs and MPs, emphasizing how size influences their physical, chemical, and optical behaviors. We detailed the challenges associated with isolating NPs from environmental samples, highlighting the limitations of traditional separation techniques when applied to nanoscale plastic particles. However, isolation is only the first step in the comprehensive analysis of NPs. Once separated, these particles must be reliably detected, identified, and quantified.

This second part of our review shifts focus to the analytical techniques used for NP detection, covering chemical identification, morphological visualization, and quantitative measurement approaches. While standardized protocols exist for the analysis of MPs, as summarised in Fig. 1, these methodologies often fail when applied to NPs. For instance techniques such as stereomicroscopy and confocal microscopy, effective for MPs, lack the resolution required for NP detection.[7] Instead, high-resolution approaches like electron microscopy or nano-infrared spectroscopy (nano-IR) are necessary.[8] Fig. 2 illustrates the lateral resolution of different microscopy techniques. If a particle's size is smaller than or comparable to the system's lateral resolution, it cannot be imaged clearly or may appear merged with noise/background. To date only advanced, low throughput, instruments can resolve nanoscale plastic particles, especially below 100 nm.

A crucial aspect of NP detection is the need for standardized protocols and validated methodologies to ensure comparability across studies. Unlike MPs, which benefit from well-established analytical workflows, as those described in ISO 24187:2023 and 5667-27:2025 for instance, NP detection remains an evolving field with significant methodological divergence.[11] This review highlights recent progress toward standardization and discusses the steps necessary to develop universally accepted procedures for NP characterization. We critically examine the strengths and limitations of currently available methods, including spectroscopy-based techniques (such as Raman and infrared spectroscopy), electron microscopy, and emerging mass spectrometry applications. Given the significant analytical hurdles in detecting sub-100 nm plastic particles, we also discuss potential advancements in technology that could improve sensitivity, reproducibility, and accuracy in NP analysis.

Several recent reviews have addressed detection of micro- and nano-plastics.[11–13] What distinguishes this review is its explicit physical chemistry lens, linking detection performance to the underlying principles of each method. Readers will (i) gain a clearer understanding of

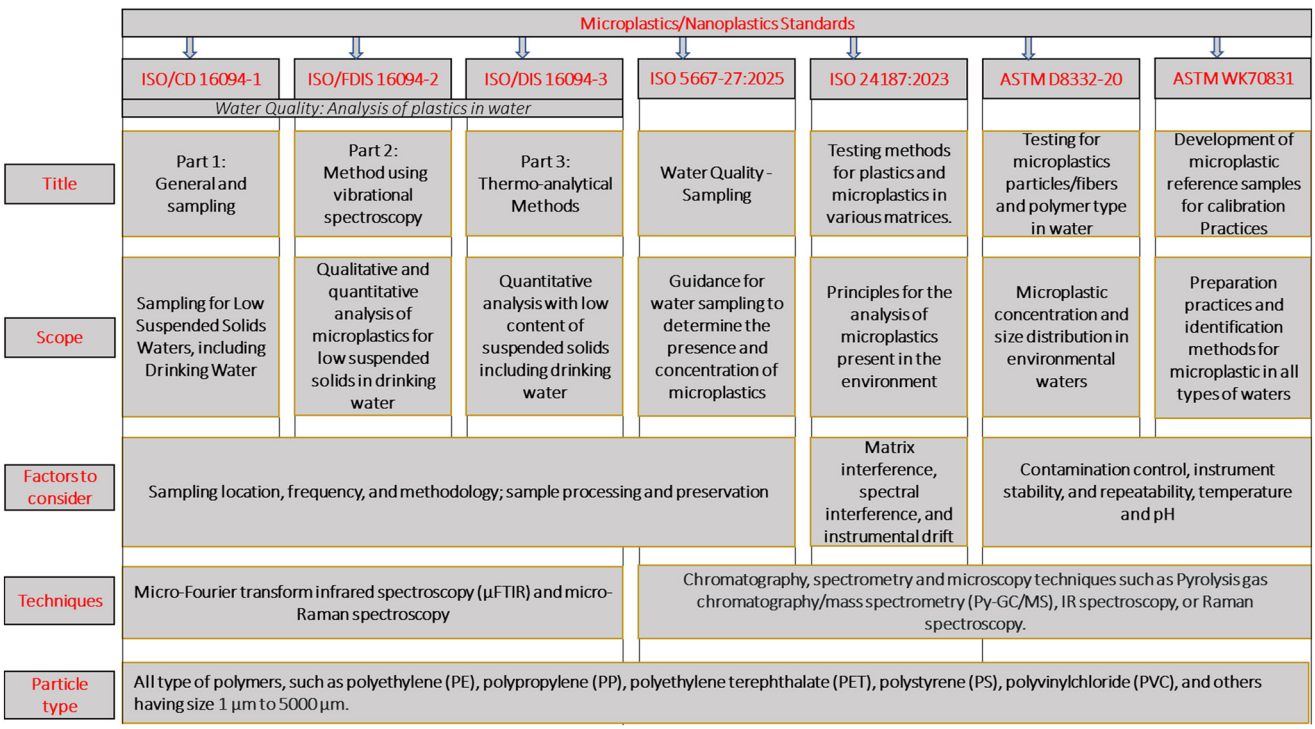

Fig. 1 Examples of existing standards relevant to microplastics (ISO/CD 16094-1, ISO/FDIS 16094-2, ISO/DIS 16094-3, ISO 24187:2023, ISO 5667-27:2025, ASTM D8332-20 and ASTM WK70831) along with their scope, techniques used, particle type with size limit and factors to consider for microplastics/nanoplastics analysis, primarily in water matrixes. Note: although some of these standards are still under development (*i.e.* those labelled DIS: draft international standard and FDIS: final draft international standard for ISO and WK: work item for ASTM, the American Society for Testing and Materials) they are all applicable to microplastics at this stage.[5,6]

This journal is © The Royal Society of Chemistry 2025

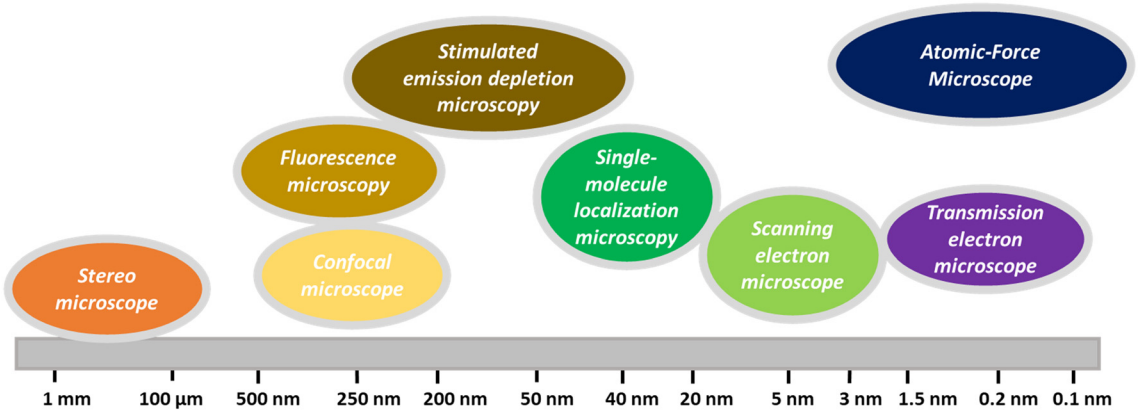

Fig. 2 Lateral resolution of microscopy techniques, determining the smallest resolvable distance between two objects and in turn the size-based limit of detection for MNPs.[1,9,10]

Published on 30 2025. Downloaded on 25.5.2026 16:41:33.

why techniques succeed or fail at the nanoscale, enabling more informed methodological choices; (ii) benefit from a comparative table that collates working ranges, detection limits, matrix compatibility, and representative references for rapid consultation; and (iii) find forward-looking discussion and roadmap suggestions to stimulate ideas on where the field may move next in addressing this environmental challenge. Ultimately, improving NP detection capabilities is essential for assessing their environmental impact, understanding their potential risks to human and ecological health, and informing regulatory frameworks.

2 Detection techniques

The detection of NPs is highly dependent on effective isolation methods, as discussed in part 1, where we explored various separation techniques and their limitations. Once isolated from their environmental matrixes, NPs need to be analytically detected to confirm their presence and/or gain

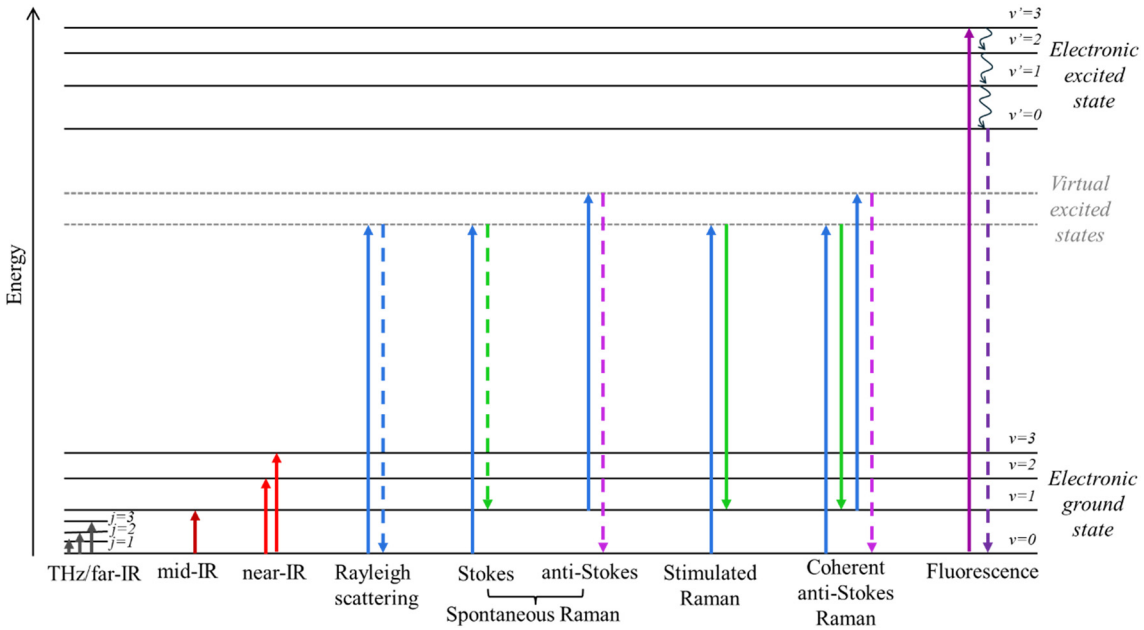

Fig. 3 A selection of absorption, emission and scattering spectroscopic methods. The solid lines indicate photons derived from a light source and dashed lines indicate photons generated in the phenomena. Far-infrared (far-IR), mid-infrared (mid-IR) and near infrared (near-IR) are absorption processes associated with rotational and phonon vibrations (far-IR), fundamental (mid-IR), overtone and combination (near-IR) vibrational transitions. Scattering can be elastic (Rayleigh) or inelastic (Raman) with energy given (Stokes) or taken (anti-Stokes) from the molecule. Stimulated Raman scattering (SRS) uses an additional laser to stimulate the scattering process. Coherent anti-Stokes Raman scattering (CARS) uses SRS to populate the vibrationally excited state which is then probed by the probe/pump laser and the anti-Stokes transition is detected. The fluorescence pathway involves absorption of the photon into an electronic excited state, non-radiative vibrational relaxation and emission from the lowest level of the electronic excited state back to the ground state. Adapted from ref. 14 with permission from Springer Nature, copyright 2016.

Published on 30 2025. Downloaded on 25.5.2026 16:41:33.

quantitative information on their shape, chemical composition, and concentration. Various detection methods that can be used to identify NPs are discussed below.

2.1 Chemical analysis: NPs polymer type identification

For the chemical identification of NPs, spectroscopic techniques are the most commonly used. Spectroscopy refers to a range of techniques that exploit how light interacts with matter to identify and characterise materials. Different type of light-matter interactions are used depending on the technique, including absorption (*e.g.* infrared spectroscopy), and scattering (*e.g.* Raman spectroscopy) phenomenon, Fig. 3.

2.1.1 IR spectroscopy. Infrared (IR) spectroscopy is an essential tool in vibrational spectroscopy that is used for the identification of molecular structure. It quantifies changes in molecular vibrational energy levels caused by the absorption of infrared radiation.[15] In plastic particles, it enables polymer identification by detecting characteristic vibrational modes of specific functional groups, such as C–H, C═O, and C–O stretches, which produce distinct absorption patterns unique to each polymer type.[14,15] For a molecule to absorb IR, its vibration must cause a change in its dipole moment. Only such vibrations are IR active. Water, for instance, is a strong IR absorber due to its strong dipole moment. When analyzing aqueous samples, the water IR absorption can lead to significant interference and obscure the signals from other analytes of interest such as NPs.[15]

Instrumental techniques for bulk IR spectroscopy analysis typically involve mid-IR radiation (fundamental vibrational transitions, 4000–400 cm^{-1}), most commonly using Fourier Transform Infrared (FTIR) spectroscopy.[15] FTIR is nowadays the most widely used experimental setup for collecting IR spectra in plastics analysis.[12] This is because FTIR offers high throughput, multiplex detection, speed, simplicity, and access to well-established, extensive spectral libraries for reliable polymer identification. FTIR analysis can be performed in three modes: transmission, reflectance and attenuated total-reflectance (ATR) mode. Transmission mode detects IR radiation penetrating through the entire sample. Transmission mode is commonly used for detecting environmental MPs but requires the sample and substrate to be IR transparent and the sample to be thin (<100 μm). While high-quality spectrum representative of the entire sample thickness can be beneficial for MP identification, total absorption can have a negative impact. For colored, dark, or opaque particles, the IR beam can indeed be partially or completely blocked, resulting in poor spectra. Reflectance mode avoids this issue by measuring the IR beam reflected off the sample. The suitability of reflectance mode depends on the sample's morphology, as surface textures can lead to light scattering and disturb the reflected signal.[12] When present, NPs themselves can behave like a fine surface roughness, with their abundance of sub-wavelength features acting as scattering centers and further reducing spectral clarity. In ATR mode, spectra are generated with the sample in close contact with an ATR crystal (such as zinc selenide). IR light passes through the crystal, creating evanescent waves that interact with the sample, allowing information to be collected. ATR mode is often used for analysing thick or highly IR-absorbent samples, such as large MPs particles (>200–300 μm).[12] In a study by Liu *et al.*,[16] it was for instance used to provide information on MP ageing by detecting surface oxidation. Ciprofloxacin was applied to polystyrene (PS) and polyvinylchloride (PVC) particles to detect differences between pristine and aged samples. Peaks characteristic of –OH were observed at wavenumbers of 3446.17 and 3437.60 cm^{-1} for aged PS and PVC, respectively, but they were not observed in the pristine samples. Moreover, the observation of carbonyl and hydroxide radicals demonstrated that MPs aging was a result of oxidation.[16] ATR mode is often the approach of choice because it requires minimal sample preparation and avoids the complex mathematical corrections needed for transmission or reflection modes. However, the ATR crystal is expensive and degrades over time. Additionally, direct contact between the crystal and the sample can lead to cross-contamination and sample loss. Furthermore, analyzing samples smaller than the crystal may result in low-quality spectra, which limits the applicability of this technique to the identification of NPs.[12]

Therefore, when examining small plastic particles, microanalysis techniques must be employed such as IR microscopy. FTIR microscopy (μ-FTIR) combines FTIR spectroscopy with light microscopy for easy analysis of small structures. The process starts with a visual examination of the sample, allowing a specific area to be selected for detailed chemical analysis. μ-FTIR enables the characterization of particles smaller than 200 μm in a contactless way. The resolution is limited by the wavelength of light and the microscope's objective. Modern μ-FTIR systems also provide chemical mapping and imaging, allowing analysis of particles as small as 10 μm with high magnification.[17] To improve μ-FTIR imaging, multi-detectors like linear array (LA) and focal plane array (FPA) can be added. These setups allow for automatic analysis of large sample areas and can gather millions of spectra in a few hours.[18] For example, it has been used to analyse the composition of teabags and their micro and nanoplastics (MNPs) leachates.[19] The results confirmed that the particles released from plastic teabags, 11.6 billion MPs and 3.1 billion NPs, shared the same composition as the original teabags, namely nylon and polyethylene terephthalate. The characteristic peaks corresponding to nylon-6,6 and poly(ethylene terephthalate) (PET) in the range of 500 to 4000 cm^{-1} were observed.[19] Another approach to improving μ-FTIR performance is the use of alternative light sources. Quantum cascade laser (QCL) – based IR systems (*e.g.* LDIR) represent the state of the art for high-throughput microplastic analysis, automating particle imaging and classification across filters at much higher speeds than conventional μ-FTIR. However, they remain diffraction-limited to ~10 μm and are therefore

 This journal is © The Royal Society of Chemistry 2025

Published on 30 2025. Downloaded on 25.5.2026 16:41:33.

not applicable to NPs, underlining the gap between MP-ready technologies and the lack of equivalent workflows for NPs. Large Area ATR-FTIR (LAATR-FTIR), combines ATR-FTIR and μ-FTIR and has been used to analyse reference MPs smaller than 10 μm. This technique involves placing an ATR crystal on the sample and scanning it in reflection mode, requiring optical contact. LAATR-FTIR benefits from ATR-FTIR's ability to provide chemical mapping and high-quality spectra. Additionally, it offers enhanced spatial resolution compared to μ-FTIR, due to the crystal's refractive index acting as a magnifying lens.[18] With this approach, LAATR units fitted with zinc selenide (ZnSe) and germanium (Ge) crystals

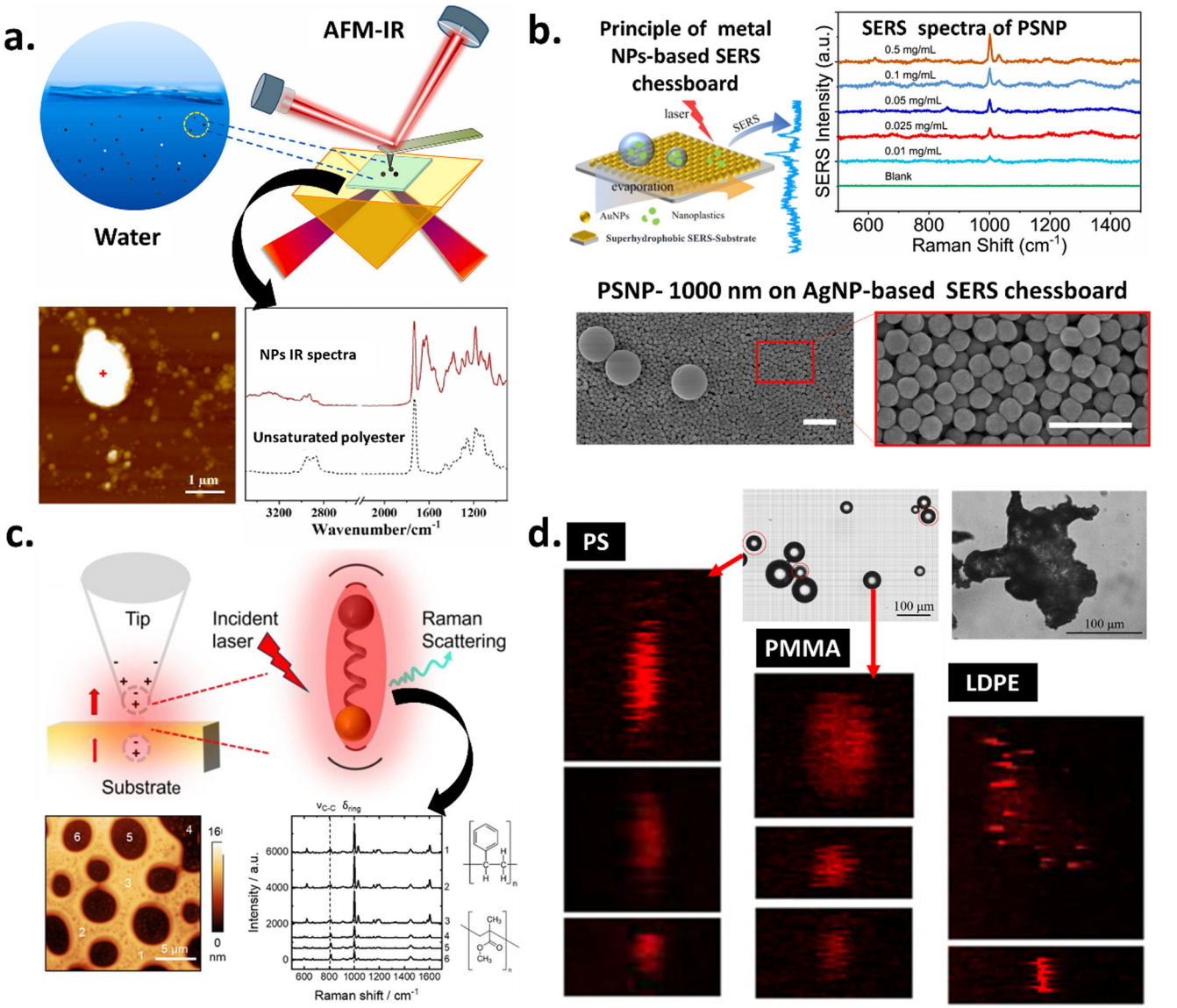

Fig. 4 a. Schematic of the AFM-IR study design and analytical set up (top) with an example of the AFM images of nanoparticles present in an environmental water, achieving ~100 nm spatial resolution, and the corresponding IR spectra acquired at the mark locations showing good match with the dashed spectra of polystyrene (PS) from the spectral library. Reproduced from ref. 22 with permission from Elsevier, copyright 2025. b. Principle of metal-NP based surface-enhanced Raman scattering (SERS) (top left), reproduced from ref. 23 with permission from the American chemical Society, copyright 2025, SEM images of a polydomain-aggregating silver nanoparticles (PASN)-SERS chessboard substrate with a 1000 nm PSNPs dispersed across the PASN substrate (scale bar: 500 nm) (bottom), along with Raman spectra measured on the PANS substrate for different size of PSNPs in tap water, reproduced from ref. 24 with permission from Elsevier, copyright 2025. c. Schematic depicting enhancement of the local electric field at the tip apex in a TERS configuration, significantly amplifying Raman signals from nearby samples (top). Reproduced from ref. 25 with permission from the American chemical Society, copyright 2025. Also shown: AFM image of a PS–PMMA (poly(methyl methacrylate)) blend with corresponding confocal Raman spectra collected at the designated points. Inset displays the chemical structures of PS and PMMA, with their characteristic Raman bands at 1001 and 813 cm^{-1} marked by dashed lines. Reproduced from ref. 26 with permission from the American chemical Society, copyright 2022. d. Bright-field and CARS images of PS, PMMA, and LDPE particles. CARS imaging detects vibrational frequencies of 3050 cm^{-1} (PS), 2940 cm^{-1} (PMMA), and 2840 cm^{-1} (LDPE). Scale bars: 100 μm. Reproduced from ref. 27 with permission from the American chemical Society, copyright 2021.

Published on 30 2025. Downloaded on 25.5.2026 16:41:33.

effectively identified small MPs down to 1.3 μm, but struggled with large MPs due to uneven contact caused by particle thickness.[18] While this one particular variant of advanced μ-FTIR, successfully identified individual MPs particles between 1.3 and 20 μm in diameter, the resolution of this instrument is generally too low to provide a unique vibrational spectra for small microparticles among larger ones, let alone NPs.[20]

Nano IR spectroscopy is a technique which integrates IR spectroscopy with atomic force microscopy (AFM) to enable chemical characterization at spatial resolutions far beyond the capabilities of traditional IR techniques. Unlike conventional IR-based methods that are limited to resolutions in the range of 5 to 10 microns, typically achieved through attenuated total reflection spectroscopy (ATR), nano IR measurements can achieve resolutions as small as 50 to 200 nanometers.[8] It is a probe-based setup wherein an AFM tip scans the sample surface, detecting local variations in IR absorption induced by molecular vibrations, Fig. 4a. A pulsed, tuneable IR source excites the sample, which then undergoes localized heating, leading to thermal expansion detected by the AFM cantilever. This localised thermomechanical response is used to generate IR spectra at the nanoscale, surpassing the diffraction limit of light. The reading integrates topographical, mechanical, and thermal analyses at the nanoscale. Combining the spatial resolution of AFM with the chemical specificity of IR spectroscopy, this instrument opens new avenues for research in NPs analysis.[8] Recent investigations have so far reported the successful detection and characterisation of different forms of NPs in environmental samples using nano IR spectroscopy. These include TiO_2-coated PP particles, NPs made of poly(3-hydroxybutyrate) (P3HB) and epoxy resins, and PS NPs down to 30 nm, Fig. 4a.[8,21,22] However, for accurate nano-FTIR analysis, sample preparation is crucial, and the method itself is expensive.

2.1.2 Raman spectroscopy. Raman spectroscopy is a form of vibrational spectroscopy that utilises the scattering interactions of light with molecules. Scattering processes are two-photon events, where the first photon hits the sample and a second photon is scattered back, these events can be elastic (no energy change, Rayleigh) or inelastic (energy change, Raman). The dominant scattering process is elastic scattering, however one in every 10^6 to 10^8 photons will undergo spontaneous inelastic scattering, where the photon will have a change in energy corresponding to a jump in molecular vibrational energy levels with the scattered photon being lower energy than the incident photon (Stokes) or higher energy than the scattered photon (anti-Stokes), Fig. 3. Monochromatic light is used to probe a sample and the difference in the energy between the incident and scattered photons is recorded to generate a spectrum with the x axis given in Raman shift (cm^{-1}) and the y-axis intensity of signal (*e.g.* counts s^{-1}). The Raman scattering process occurs when vibrations exhibit a change in polarizability (deformation of electron cloud/orbital during the vibration) which tends to occur to a greater extent in molecules with π-bonds and delocalised systems, such as the styrene groups of polystyrene. In contrast, water is a poor Raman scatterer and as such Raman spectroscopy can be undertaken for aqueous systems with minimal interfering water signals, unlike FTIR.[15,28]

To enable small sample volumes and high lateral resolution, Raman spectroscopy can be coupled into microscopes (Raman microscopy or Raman micro spectroscopy). The sample volume measured is governed by the diffraction limited spot size which is dependent on the wavelength of light and the numerical aperture of the objective. The visible wavelengths of light typically used can provide smaller spatial resolution compared to μ-FTIR spectroscopy. Raman microscopy can achieve a spatial resolution as low as 1 μm and even below (approximately 300 nm) depending on the wavelength and objective setup utilised.[1] However competing phenomenon, such as fluorescence, can mask the relatively weak Raman signals, in such instances longer wavelengths are often utilized. One downside to this is the $I_R \propto \nu^4$ relationship between Raman signal intensity (I_R) and excitation frequency (ν) with longer wavelengths resulting in reduced signal intensity.[29] This trade-off is particularly acute for NPs, where emissive plastics often require longer excitation wavelengths to avoid fluorescence, resulting in intrinsically weaker Raman signals and reduced spatial resolution.

PS-NPs ranging from 30 to 600 nm were identified using Raman imaging combined with an image algorithm analysis that relied on distinguishing the laser spot, the pixel size/image resolution, the NPs size/position (within a laser spot) and the Raman signal intensity.[30] Raman microscopy has also been used to characterize paint-polishing dust samples collected from a driveway after manually polishing a vehicle's poly-acrylic clear coating. Analysis of the dust samples estimated this polishing process to be responsible for the generation of billions to trillions of MPs/NPs, with sizes ranging from approximately 7 μm down to 200 nm.[31] Raman imaging has also been used in association with 2D optical tweezers or coupled with asymmetrical flow field-flow fractionation (AF4), to identify irregularly shaped, aggregated, and polydisperse NPs.[32] The main drawback of this process was that non-homogeneous hot-spot densities (uneven concentrations of electromagnetic field enhancement) and non-uniform distribution of NPs over the substrate caused poor reproducibility.[33] This limitation could be addressed by using a capture material promoting homogeneous adsorption densities. Other limitations associated with Raman include size-range detection and penetration depth. For instance, analysing polished silicon wafers with different laser wavelengths reveals varying penetration depths—12 μm at 785 nm, 3 μm at 633 nm, and 0.7 μm at 532 nm.[34] In the UV range, penetration depth can drop to 5–10 nm.[34] Nonetheless Raman has the advantages over XPS and FTIR to cover a wider spectral range, to have higher sensitivity to nonpolar functional

 This journal is © The Royal Society of Chemistry 2025

Published on 30 2025. Downloaded on 25.5.2026 16:41:33.

groups, lower water interference and narrower spectral bands.[31]

Surface-enhanced Raman spectroscopy (SERS) is a version of this technique that significantly amplifies the Raman signals of molecules by several orders of magnitude.[35] Such amplification is particularly critical for NPs, whose small volume makes conventional Raman signals intrinsically weak and prone to baseline interference. It involves adsorbing molecules on colloidal metal nanoparticles or rough metal surfaces, typically silver or gold,[23,35] leading to higher scattering efficiencies, Fig. 4b. The proposed enhancement mechanisms include electromagnetic (EM) and chemical enhancement (CE) theories. EM enhancement results from the unique properties of metal nanoparticles, such as surface plasmon oscillations, which concentrate light energy and increase Raman scattering.[35] CE involves interactions between probe molecules and a metal surface, facilitating changes in electronic structure and electrical charge sharing, thereby strengthening and sensitizing the Raman signal and contributing to overall enhancement.[35] Using SERS, PSNPs of varying sizes (30, 100, 200, and 1000 nm) were examined on Ag nanoparticles, Fig. 4b.[24] In the presence of potassium iodine, acting as coagulant, this approach showed a marked degree of sensitivity, particularly in the case of 100 nm PSNPs, where a detection limit of 6.25 μg mL^{-1} was achieved. The method was successfully applied to real-world lake water samples, detecting more than 87.5% of various NPs sizes and concentrations.[36] SERS also proved to be an efficient tool for NPs (PS, PE, and PP) $<$ 500 nm in both pure water and seawater. Notably, PS, PE and PP NPs down to 100 nm exhibited strong signals compared to MPs due to their higher surface area.[37] This highlights that nanospecific properties can sometimes enhance detection, as the increased surface-to-volume ratio improves scattering efficiency relative to larger MPs. Moreover, in biological samples, SERS has been used to visualize fluorescently labelled NPs involved in bio-nano interactions. Unfortunately, this approach is prone to autofluorescence which led to low quality spectrum as the fluorescence masked the Raman signal. To overcome this drawback and improve the accuracy of NP visualization, researchers have proposed a novel near-infrared (NIR) SERS labelled NP with anti-interference properties. Using this technique, the uptake of NPs in Zebrafish was successfully confirmed without autofluorescence.[38] Despite this progress, it remains crucial to investigate the nature of this interfering signal and how it is influenced by factors such as the size, surface charge, structure, the presence of additive, dyes or the chemistry of the NPs under study.

Tip-enhanced Raman spectroscopy (TERS) is another variant of Raman, which like SERS aims to amplify the signal. TERS uses scanning tunnelling microscopy to scan a plasmonic metal nanostructure across a sample surface to locally amplify the field, Fig. 4c.[25] During TERS examinations, the nano-enhanced probe tip is placed above the sample and a laser is used to stimulate the localized surface plasmon resonance (LSPR) of the particle of interest. The LSPR, a synchronized oscillation of conduction electrons, significantly amplifies (by a factor of 100–1000) the electric field in the immediate vicinity of the nanoparticle, resulting in enhancement factors of up to 10^8.[39] TERS allows for precise chemical analysis with a spatial resolution of around 30–50 nm. In certain cases, such as with carbon nanotubes, the resolution can even reach as low as 1.7 nm when using STM. TERS has the potential to offer detailed nanoscale chemical information on NP particles.[40] However, studies using TERS have so far focused on the analysis of polymer-blend thin films, rather than individual particles. In PMMA and PS polymer blend, TERS used in combination with XPS provided information on phase separation with vertical resolution lower than 10 nm,[26] while lateral resolution below 100 nm were achieved for PS and polyisoprene (PI) blends, Fig. 4c.[41] Therefore, further exploration is needed to determine the extent to which this highly promising technique can be applied in the field of NPs.

2.1.3 X-ray photoelectron spectroscopy. X-ray photoelectron spectroscopy (XPS) is used to obtain information regarding binding energies of specific electron orbitals by irradiating samples with an X-ray radiation.[42] XPS is a surface-sensitive method that provides much higher resolution in the *z*-direction compared to FTIR or Raman. However, the lateral resolution of XPS (or spot size) is still ~10 μm. XPS is a powerful tool to study the chemical composition of the top 10 nm of a surface.[42] The X-ray radiations emitted by photoelectrons in XPS analysis provides information about the bonding environment of specific elements. For instance, high resolution C1s spectra of PSNPs can be used to confirm the presence of aromatic carbon and hydrocarbon groups within the C1s envelop with components at ~284.3 and 284.7 eV, respectively.[43] C1s XPS spectra has also been used to confirm the chemical composition of PS and PENPs in cosmetics and the presence of polymeric substances in wastewater treatment plant microorganisms.[20] XPS is capable of detecting surface oxidation in NPs through changes measured in the oxygen high resolution spectrum.[43] Surface functional group changes in pristine PS and aged PS nanoparticles were investigated using XPS. The analysis revealed decreasing C/O ratios with irradiation time, as seen in pristine PS (C/O ratio: 2.48), PS aged for 12 hours (C/O ratio: 2.24), and PS aged for 24 hours (C/O ratio: 2.07). Results aligned with FTIR findings, and high-resolution scans identified increased C–O, C═O, and O–C═O bonds in the aged PS, confirming the oxidation of PSNPs during aging.[44] However, XPS is a very expensive technique to use on a routine or commercial basis due to the cost of the instrument itself and it is therefore typically only used for research purposes.[45]

2.1.4 Non-linear spectroscopic methods. Recent studies have demonstrated that non-linear optical methods, specifically techniques like stimulated Raman spectroscopy (SRS), coherent anti-Stokes Raman scattering (CARS), and two-photon excited autofluorescence (TPEAF), could play a crucial role in the detection and characterization of NPs.[46,47]

Published on 30 2025. Downloaded on 25.5.2026 16:41:33.

The hyperspectral imaging capabilities of SRS allow for precise chemical characterization of NPs, aiding in the differentiation of complex mixtures and the study of particle heterogeneity.[46,47] SRS enables high-resolution, 3D imaging of NPs down to 50–100 nm. This technique has proven effective in identifying various types of NPs such as PS, PMMA and PE in environmental and biological samples, including bottled water, atmospheric particles, and human lung tissues, revealing a much higher abundance of these tiny particles than previously detected by traditional methods.[46–48] However, SRS requires extensive spectral libraries and resolving overlapping signals is complicated, which makes the identification of NPs in complex matrices difficult.[46,47]

Coherent Anti-Stokes Raman Scattering (CARS) microscopy is another technique used to increase the Raman signal, which could be proved useful for NP detection due to its non-invasive, label-free imaging capabilities, coupled with high sensitivity and chemical specificity. To date, CARS has been used to identify and classify PMMA, PS, and LDPE MPs, even in challenging environments like continuous water flow, without the need for labour-intensive sample preparation, Fig. 4d.[27] This could make CARS particularly useful for real-time monitoring and *in situ* analysis of NP pollution, should high enough resolution be achieved. The integration of CARS with other techniques, like two-photon excited autofluorescence (TPEAF), was shown to enhance its ability to differentiate between plastic and organic particles, providing high spatial and temporal resolution.[27] However, like most advanced spectroscopic techniques, the practical application of CARS faces significant technical barriers, in terms of miniaturization and integration of advanced features without sacrificing performance and acquisition times. Though the field is rapidly progressing and could soon see Raman imaging become a tool of choice for NPs identification, as reviewed in details elsewhere.[49]

IR is widely used for MPs but lacks the resolution needed for NPs unless applied as nanoIR, which is a new and promising technique, though still very slow and limited to specialised laboratories. Raman is more accessible: even relatively common models can achieve <1 μm resolution, and with confocal mapping they can also provide imaging capabilities. This means size and shape information can be obtained alongside polymer identification in a single instrument. When newer approaches such as faster mapping, TPEAF or SERS substrates are used, both resolution and throughput improve further. SERS in particular is attractive because it can be implemented on existing Raman systems with appropriate substrates, unlike other advanced variants that require major hardware upgrades. In all cases, relevant spectral libraries, automation and faster acquisition remain critical if these methods are to become routine, as demonstrated by LDIR for MPs. XPS is probably best regarded as a niche method: while it provides valuable information on surface chemistry and oxidation states, its lateral resolution is too low to probe individual NPs, so meaningful data can only be obtained on beds of particles with similar properties.

2.2 Morphological analysis: techniques for NPs visualisation

2.2.1 Atomic force microscopy. Atomic Force Microscopy (AFM), a form of scanning probe microscopy, is one of the most effective techniques for imaging and characterising surfaces at the nanoscale with a lateral resolution of 2 nm, and vertical resolution down to 0.1 Å.[50,51] AFM operates with a sharp tip affixed to a flexible cantilever which engages with the sample surface. Minute deflections of the cantilever are tracked by a photodetector measuring reflected light, while a piezoelectric scanner moves the tip or sample in tiny steps to reconstruct the surface topography. A feedback mechanism continuously modifies the tip's elevation to ensure consistent engagement with the surface, facilitating the creation of a three-dimensional map.[51] It can be operated in contact mode, where the tip remains in constant contact with the surface while the cantilever deflection is maintained at a steady state or in tapping mode. Here the cantilever oscillates close to its resonance frequency minimising damage to fragile or soft specimens. Tapping mode is therefore optimal for polymers, biological samples, or NPs. It is this fundamental principle that both nanoIR and TERS rely on for tip positioning to achieve their nanoscale resolution. Though AFM can also be used on its own to image NPs. In addition to imaging, advanced AFM modes can quantify elastic modulus, adhesion, conductivity, and surface potential.[51] AFM studies on NMPs (0.5–10 μm) showed that natural aggregates have higher roughness and surface area than lab-aged particles, indicating greater adsorption potential. Surface analyses of aged polyethylene (PE) lobster trap tags and polypropylene (PP) fragments confirmed severe fragmentation and degradation, influenced by colorants and environmental factors. These results highlight AFM's ability to provide high-resolution morphological and mechanical insights beyond what chemical analysis alone can reveal.[52,53] On the downside, image acquisition and processing can be laborious and the scanned areas are so small (typically 100 μm^2 maximum) that AFM images may not statistically represent the entire sample, particularly in heterogeneous materials. Also the vertical range seldom surpasses 5 μm which makes imaging highly textured or stacks of nanoparticles challenging. For NP analysis care should be taken for the particles to be strongly adsorbed onto the surface of tip-induced artefacts may manifest in the data. Delicate or fragile specimens are susceptible to tip-sample interactions, especially in contact mode.[50,51] Nonetheless, when combined with techniques like TERS or Nano-IR, AFM offers a more holistic understanding of complex materials, such as NPs, providing information not only on their morphology and surface roughness but also their chemical and physical properties, which makes them intrinsically multimodal detection techniques.

 This journal is © The Royal Society of Chemistry 2025

Published on 30 2025. Downloaded on 25.5.2026 16:41:33.

2.2.2 Scanning electron microscopy. Scanning electron microscopy (SEM) can be used to get quantitative information about NPs size, shape, surface morphology, and aggregation state[2] with resolution below 3 nm. When equipped with EDX detectors (Energy Dispersive X-ray-Spectroscopy) SEM can also provide data about the chemical composition of the samples.[2] In SEM, the sample is scanned with an electron beam. When the electrons from the beam come in contact with the atoms in the sample, they experience elastic and inelastic scattering which result in the production of backscattered and secondary electrons, X-rays and other signal that are processed by the instruments detectors and rendered into a high-resolution image of the sample's surface features. The advantage of SEM is its high resolution with 3 nm size limit, the ability to acquire images within minutes and to survey rather large areas of samples.[2] SEM is typically used to visualise the actual size and shape NPs, such as the PS and PMMA nanospheres (50 nm, 100 nm, and 500 nm) shown in Fig. 5a. The size distribution observed are often compared to DLS data to confirmed or infirmed consistency with commercially reported sizes.[54] SEM analysis can also be used to observe adsorption of NPs onto the surface of other compounds,[20] or to study NPs morphological stability, for instance when subjected to hot water during takeaway food consumption, high-temperature sterilization, and other simulated food scenarios.[55]

SEM offers high-resolution imaging with excellent surface sensitivity, providing detailed static images. However, its reliance on conductive coating and a vacuum environment, along with the potential for electron beam-induced sample damage, and low throughput makes its application to routine analysis unpractical.

2.2.3 Transmission electron microscopy. Transmission electron microscopy (TEM) is commonly used to visualise nano-sized particles, providing high-resolution images and chemical information at the atomic scale.[56] TEM's ability to provide detailed information about NPs relies on an electron beam generated from a thin foil within the instrument and directed at the sample. As the beam interacts with the sample, electrons ae scattered and subsequently detected to create a detailed image. Operating at higher voltages than SEM (beyond 80 kV), TEM can be coupled with EDS and image software, allowing the identification of elemental composition in nanoparticles, with the software aiding in image processing. One of the only study reporting on the use of TEM for NP analysis in environmental samples (Fig. 5b) focused on snow samples.[58] Another laboratory based study used TEM to analyse the morphology of PS NPs and CeO_2 NPs, revealing a spherical shape with an average diameter of approximately 50 nm confirmed with DLS for PS–Bare, PS–COOH, and PS–C_2H_2O, and around 80 nm for PS–NH_2 and PS–SO_3H.[56,59] Despite TEM's widespread use for characterizing the morphology and size of nanomaterials, its application in detecting NPs is limited. The amorphous nature and elemental composition of polymers present an intrinsic challenge in

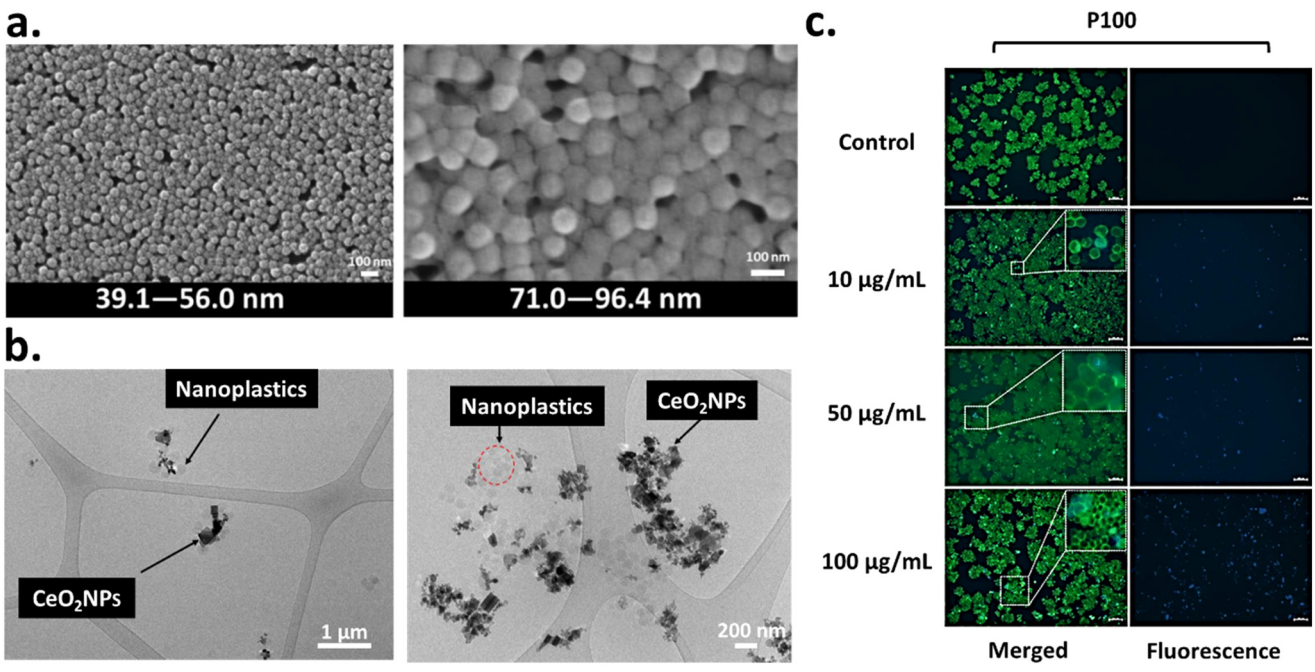

Fig. 5 a. Scanning electron microscopy (SEM) images polystyrene (PS) and poly(methyl methacrylate) (PMMA) nanoplastics. Reproduced from ref. 54 with permission from the American Chemical Society, copyright 2021. b. Transmission electron microscopy (TEM) images showing cerium oxide (CeO_2) nanoparticles and PS NPs in environmental samples collected from seawater (left) and lake water (right). Reproduced from ref. 56 with permission from Elsevier, copyright 2020. c. Fluorescence microscopy images of macrophages (cytoskeleton actin is labelled in green) exposed to blue-labeled 100 nm PS NPs at concentrations of 10, 50, and 100 µg mL^{-1} for 48 hours, highlighting cellular uptake and dose-dependent interactions. Reproduced from ref. 57 with permission from Elsevier, copyright 2024.

Published on 30 2025. Downloaded on 25.5.2026 16:41:33.

TEM analysis as the ineffective elastic interaction of organic elements with the electron beam results in weak contrast. As with SEM, conductive or high-Z samples provide much better contrast, making plain polymer NPs intrinsically difficult to image. Enhancing detection efficiency requires staining NPs with heavy elements; when these stains are purposedly added they may impact the chemical composition and structure of the polymers.[9] However, in the case of environmental NPs, which are often reported to adsorb heavy metals or form complexes with inorganic colloids, this very contamination may enhance electron contrast and thereby improve detectability.

2.2.4 Fluorescence. Fluorescence labelling of NPs to track them in the environment and in living organisms has been the focus of multiple studies, Fig. 5c. This is the only approach that actively uses the nano-specific physical properties of NPs to enable their detection. Specifically, fluorescence-based methods build on the hydrophobic nature of most hydrocarbon-derived plastics and the enhance surface reactivity of NPs, which together promotes the adsorption of lipophilic fluorescent dyes. This strong surface affinity is advantageous for NPs compared with MPs, where dye uptake is often less efficient. Nile Red (NR) is the most widely used dye for MNPs detection because of its high fluorescence intensity, fluorescence quantum yield (Φ_f = 0.42) in non-polar media,[60] high adsorption, and solvatochromic properties, which allow it to effectively stain various plastic polymers. NR has been successfully applied across a range of environmental samples, including sediments, water, and biota, thanks to its ability to categorize MNPs based on their hydrophobicity. However, its use is not without challenges; NR can exhibit weak signals with certain plastics and faces issues with staining fibers. Rhodamine B (RhB) also shows promise as a NP dye, particularly for PS microspheres, though it is limited by toxicity and partial staining of smaller particles. Safranine T (ST) and Eosin B have been used with some success, but their applications are hindered by potential harmful effects and limited testing in complex environmental matrices.[10]

However, due to dye leakage, photobleaching, and organism autofluorescence, this approach often shows poor accuracy and false-positive results.[10] Another significant limitation of fluorescence-based methods is the non-specific labelling of other hydrophobic particulate matter and high background fluorescence levels, which can also lead to false positives.[10] Pre-treatment steps, such as separation or digestion techniques, are crucial to minimize interference from suspended solids and organic matter. Despite these precautions, the detection of NPs presents additional challenges compared to MPs due to their smaller size, which requires highly sensitive and specific staining techniques. Current research emphasizes the need for optimized staining protocols and the development of new fluorescent dyes or counterstaining methods to enhance the accuracy and efficiency of fluorescence-based detection of NP in environmental and biological samples.[10,57]

SEM and TEM provide the highest resolution and are unrivalled for shape details at the nanoscale, but the weak contrast and charging artefacts of pristine polymer NPs limit their value as a standalone tool. Interestingly, environmental NPs that bind metals or mineral colloids may yield stronger EM signals than laboratory standards, suggesting a potential advantage if exploited carefully. In practice, however, concentrating environmental NP samples sufficiently to "find" particles without introducing excessive mineral artefacts remains a challenge, as discussed in part I of this review. Fluorescence microscopy, by contrast, is significantly cheaper and is the only imaging approach that directly leverages nano-specific surface properties, making it a realistic high-level screening option. In both cases, reliable identification requires pairing with spectroscopic methods.

2.3 Population analysis: size distribution and concentration

2.3.1 Dynamic light scattering. Dynamic light scattering (DLS), also known as photon correlation spectroscopy or quasi-elastic light scattering,[61] is an analytical technique used to measure the size of particles and macromolecules by measuring their Brownian motion in a dispersion and determining their hydrodynamic radius. Smaller particles move or diffuse more rapidly than larger ones, with the rate of Brownian motion quantified as the translational diffusion coefficient D. The hydrodynamic size determined by DLS is defined as the size of a sphere that diffuses at the same rate as the particle being measured, including the core particle and anything strongly bound to its surface, such as ions, adsorbed molecules. DLS involves illuminating particles with a laser to measure diffusion rates.[61] Particles that are not moving show a consistent level of scattered light intensity. However, when diffusion occurs, there are variations in the scattered light that are proportional to the size of the particles and how fast they are moving. These rapid light-scattering signal fluctuation are analysed over time through autocorrelation functions, where a faster decay indicates smaller, more mobile particles. The Stokes–Einstein equation relates this diffusion behaviour to the particle's hydrodynamic diameter, allowing the size of nanoparticles to be estimated from DLS data:

$$d_H = \frac{kT}{3\pi\eta D} \quad (1)$$

where d_H is the hydrodynamic diameter, k is Boltzmann's constant, T is the absolute temperature, η the viscosity of the medium and D the diffusion coefficient. For accurate calculations and particle sizing, the solvent viscosity and temperature must be known, but this is not always the case.

While DLS offers quick and non-invasive measurement of particle sizes its accuracy can be compromised by contaminants, viscosity, and temperature fluctuations, particularly when analysing non-spherical shapes.[2,20] DLS was used to determine the stability of 0.01, 0.1, and 1 g L^{-1} solutions of PS and PMMA NPs in ultrapure water. Particles

 This journal is © The Royal Society of Chemistry 2025

Published on 30 2025. Downloaded on 25.5.2026 16:41:33.

having a mean diameter of 142.70 ± 5.53 nm (PS) and 96.46 ± 5.52 nm (PMMA)[62] were detected. DLS was also used to investigate the aggregation of dissolved organic matter in the marine environment and how it formed particulate organic matter, in the presence of 25 nm PS/PMMA. The study concluded that this induced aggregation may pose a potential hazard to the marine carbon cycle.[63]

2.3.2 Nanoparticle tracking analysis. Just like DLS, Nanoparticle Tracking Analysis (NTA) is used to determine the size of particles within the range of 10 nm to 1000 nm. It is a cutting-edge method that harnesses particle scattering and employs an optical microscope to observe the Brownian motion of particles, illuminated by laser light. This high-precision approach records the motion of particles frame by frame through a high-sensitivity camera, which enable concentration measurements.[64]

Unlike Dynamic Light Scattering (DLS), NTA provides accurate measurements even in the face of polydisperse nanoparticles suspensions. The key lies in NTA's capability for single particle tracking, enabling real-time analysis and superior resolution of overlapping size distributions. In practical terms, this translates to more precise size distribution measurements, especially in polydisperse samples.[65] For instance, Filipe *et al.* conducted a comparative study using both NTA and DLS, focusing on PS submicron- and nanoparticles (60–1000 nm). The results highlighted NTA's suitability to accurately characterize individual particle populations within polydisperse samples, a task that proved challenging for DLS.[65] Also, it can be useful for secondary NPs, where the presence of aggregates or agglomerates can complicate size analysis using traditional DLS.[20] For instance, this method achieved approximately 90% recovery for various fluorescently labelled NPs, namely, 76 nm PVC, 100 nm PS–COOH, and 750 nm PS.[66] NTA was used to estimate the concentration of poly(ethylene terephthalate) (PET) NPs in commercially bottled drinking water, with a concentration of approximately 10^8 particles per mL.[67] NTA was employed to detect particle sizes and number concentrations in teabag leachates. The study revealed that the particles in the leachates exhibited spherical or elliptical shapes, with sizes ranging from 100 to 300 nm. NTA measurements reported hydrodynamic sizes of 156, 173, and 165 nm for PET/PE, PLA, and PET teabag leachates, respectively. The NTA-derived particle number concentration for the blank experiment was $3.5 \pm 0.6 \times 10^7$ particles per mL, significantly lower than the teabag groups.[68] In another study, the physical degradation of nanosized PS particles from MPs *via* rotation mixing, shaking, and flowing was investigated. The NTA analysis showed that the resulting particles had an average size of 204.0 ± 2.1 nm. Additionally, the shaking samples had fewer aggregates compared to the rotating mixing and flowing samples.[69] One of the limitation of NTA is its rather narrow operating range: it can only accurately measure the concentration of particles in the range of 10^7–10^9 particles per mL.[65] In samples that are too concentrated overlapping particle tracks can distort the results. If it is too dilute, the particles counts are too low for reliable statistical analysis. Also like other scattering based technique (*i.e.* DLS) NTA is biased towards larger particle, which are overrepresented in number-based distribution because they scatter more light.

2.3.3 Flow cytometry. Flow cytometry is a technology that is not typically categorized as a spectroscopic technique, though it does incorporate principles of light interaction similar to those used in spectroscopy. Flow cytometry provides rapid multi-parametric analysis of single particles as they flow past single or multiple lasers while in suspension.[70] Flow cytometers utilize lasers as light sources to produce both scattered and fluorescent light signals. The light scatter by each particle is measured in two different directions, the forward direction (forward scatter or FSC) which can indicate the relative size of the particle and at 90° (side scatter or SSC) which indicates the internal complexity or granularity.[70] Flow cytometry/imaging is mainly utilized to characterize size distribution, particle count, and sometimes surface charge.[70] In face masks, PP particles of sizes >100 nm were quantified by flow cytometry. The FSC was set at the lowest voltage (photomultiplier tube (PMT) = 200 V) to maximize the size range of detectable particles, while the SSC was set at 350 V to obtain a better resolution for sizing submicrometric particles.[71] Fluorescent staining and high-throughput flow cytometry were used to identify and quantify nine polymers in freshwater: PS; PE; PET; HDPE; LDPE; PVC; PP; nylon (PA); PC. All nine plastic types were stained with 10 mg mL^{-1} Nile red in 10% dimethyl sulfoxide for 10 minutes. PS, PE, PET, and PC were clearly identified, but PVC, PP, PA, LDPE, and HDPE were partially obscured by Nile red aggregation and precipitation.[72] Mixtures of PS particles that varied in size (500 nm to 5 μm) and varied in labelled populations were analysed and sorted into distinct populations reaching sorting efficiencies >90%.[73] The lowest spatial detectable limit for plastic particles was 200–500 nm.[72] However, newer instruments are being developed that lower the size detection limit of flow cytometry down to ~30 nm. Referred to as nano flow cytometers, these systems incorporate enhanced side scatter optics (*e.g.* violet laser excitation combined with a high numerical aperture lens and narrow collection angle to improve detection of weakly scattering particles), a narrower core stream to efficiently centre small particles, and high-sensitivity detectors such as avalanche photodiodes (APDs) or low-noise photomultiplier tubes (PMTs). These features make nano flow cytometers well-suited for detecting low-scattering NPs, which are often missed by conventional flow cytometry.

DLS, NTA, and flow cytometry are the only techniques that directly analyse particles in suspension, making them the natural first choice for liquid samples, especially relatively clean water (*e.g.* bottled or tap). They exploit nanospecific behaviours such as Brownian motion and scattering to deliver high-throughput, real-time size distributions, and in the case of NTA and flow cytometry, particle numbers. DLS instruments can additionally measure particle surface charge (zeta potential), which is highly relevant in studies of stability and cytotoxicity. Outputs from all three methods rely on

Published on 30 2025. Downloaded on 25.5.2026 16:41:33.

assumptions of spherical particle shape and known refractive index, and are easily skewed by bubbles, aggregation, or low particle numbers. The operating concentration ranges for DLS and NTA are narrow, and readings outside this window may appear valid which can be misleading without careful calibration. Nonetheless these methods have the advantage to be widely available in materials and chemistry laboratories (though less so in environmental sciences) and, when used critically, provide valuable bulk screening tools before more definitive chemical identification.

2.4 Quantification in mass

2.4.1 Pyrolysis-gas chromatography-mass spectrometry. Py-GC-MS is a chemical analysis technique where a sample is heated in the absence of oxygen, causing it to break down into smaller, stable fragments. This process, known as pyrolysis, allows researchers to analyse the components of environmental samples. Unlike traditional GC-MS methods, Py-GC-MS doesn't require complex sample preparation like extraction and dilution. It can effectively identify a wide range of polymers and composite materials, making it particularly useful for studying micro- and nano-plastic pollution in the environment. In an early study on NPs in oceanic waters, Ter Halle *et al.*[74] utilized ultrafiltration for sample concentration, analysing the resulting colloidal fraction with Py-GC/MS. Despite determining the relative abundance of the three major polymers through chemometric principal component analysis of aromatic pyrolyzates, quantification by weight was not undertaken.[74] Wahl *et al.*, employing py-GC-MS, identified PE, PS, and PVC NPs in water extracts from agricultural soil samples.[75] Additionally, Materić *et al.* reported low concentrations of PET NPs (5.4–27.4 ng mL^{-1}) in surface snow samples from the Austrian Alps using Thermal-Desorption Proton-Transfer-Reaction Mass Spectrometer (TD-PTR-MS).[76] However, these methods have been only tested at laboratory scale and are difficult to be applied in more complex field samples that contain other particles. Once again, this approach relies on the development of selective separation steps for environmental matrixes reduction, such as those established by Okoffo and Thomas.[77]

2.4.2 Thermogravimetric analysis. Thermogravimetric analysis (TGA) is a destructive analysis used for the identification and quantification of polymers by tracking the weight change of a particle subjected to increasing temperature. When utilizing thermal analysis for the assessment of polymer particles, the initial procedure entails exposing the sample to heat. As the temperature increases, the sample efficiently absorbs a substantial quantity of heat, leading to a progressive transformation of the polymer components from a solid state to either a liquid or gaseous state. Consequently, an endothermic peak emerges at a specific temperature. By studying the distinctive thermograms of polymers, it becomes possible to analyse the composition and type of polymers along with their additives. This is feasible due to the varying thermal stability exhibited by different polymer types.[78] TGA cannot identify specific sample components, lacks structural and morphological data, and does not provide kinetic information. However, combining TGA with complementary techniques like Differential scanning calorimetry (DSC), FTIR, or Py-GC/MS has been used to provide a more comprehensive analysis of the sample's thermal behavior and composition. Dümichen E. *et al.* analysed unknown polymers (PP/PE/LDPE) by coupling TGA with thermal desorption gas chromatography mass spectrometry (TDU-GC-MS).[79] Another group coupled TGA with FTIR to identify PE, PP, PS, PET, PVC in sea water and soil samples.[80] There is no lower size limit of detection for thermal analysis, which can be an attribute when it comes to quantifying NPs. However, the challenge then lies in sample preparation, as extracting and concentrating NPs above the instrument limit of mass detection (LOD) may require very large volume of stock sample.

2.4.3 Matrix-assisted laser desorption/ionization time-of-flight mass spectrometry. Matrix-assisted laser desorption/ionization time-of-flight (MALDI-TOF) is a mass spectrometry technique that employs MALDI as an ion source and TOF detection as the mass analyser. MALDI works in three steps to ionize the sample: (1) the sample is mixed with a matrix material consists of crystallized molecules (*e.g.*, sinapinic acid and 2,5-dihydroxybenzoic acid) and applied to a target plate, (2) the matrix-sample mixture is irradiated with a pulsed laser, causing desorption from the target plate, and (3) the analyte molecules are ionized within a hot plume of ablated gases and then analysed by Mass Spectrometry (MS). TOF MS determines the ions' m/z (mass to charge) ratio by accelerating ions in an electric field of known strength and length. The time taken for ions to fly through a fixed distance depends on the velocity of the ions and is further used to calculate the m/z ratio and identify the ion.[81] MALDI-TOF can detect various synthetic polymers.

MALDI-TOF-MS achieved the detection and characterization of plastic components present in trace amount in various environmental matrixes.[83] This technology was for instance used in the analysis of MNPs in biological samples to identify and quantify micrometrics, as depicted in Fig. 6.[83] In another instance, MALDI was used for the ultra-trace quantification of micro and nanoplastics (MNPs) in snow and water. The combination of nanostructured laser desorption/ionization time-of-flight mass spectrometry (NALDI) with MS allowed for highly sensitive detection, even at the picogram level.[58] This high sensitivity makes MALDI a versatile method for direct quantification of NPs and molecular identification of the polymer types. Though this approach does not provide morphological data (size, shape, distribution) and would need to be complemented by imaging techniques to achieve comprehensive characterisation.

Thermal and mass-spectrometric techniques such as Py-GC-MS and MALDI-TOF are widely used for polymer identification and quantification, particularly in complex matrices such as soils and sediments, where optical and spectroscopic methods are limited by light scattering and

 This journal is © The Royal Society of Chemistry 2025

Published on 30 2025. Downloaded on 25.5.2026 16:41:33.

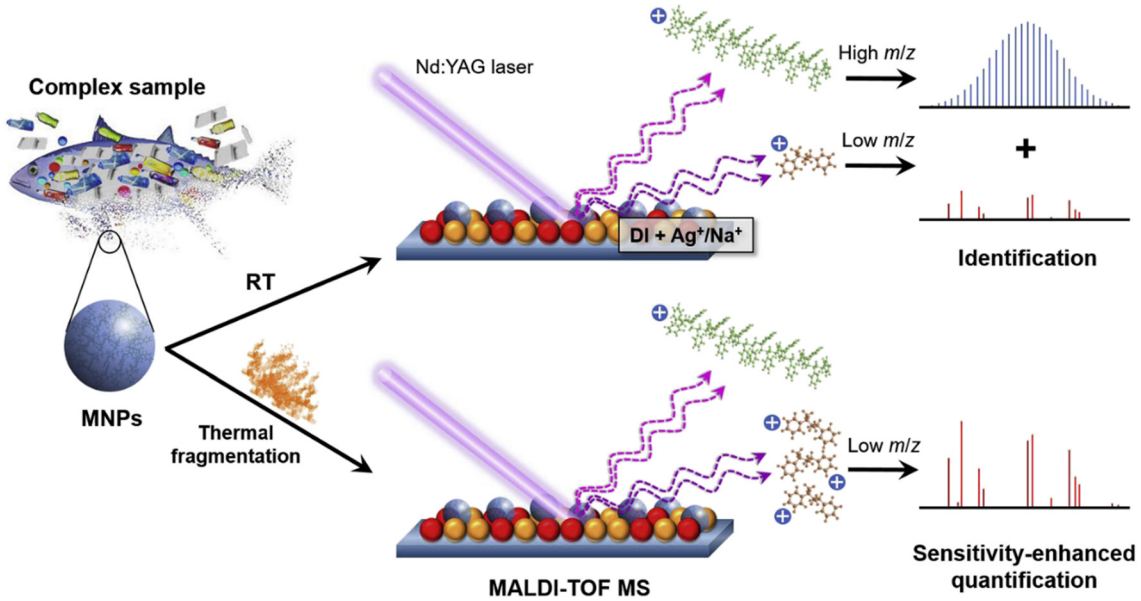

Fig. 6 Schematic illustrating the procedure and underlying mechanism for defining and quantifying the thermally assisted ionisation of PS MNPs using MALDI-TOF MS at room temperature. Reproduced from ref. 82 with permission from Elsevier, copyright 2020.

matrix opacity. Py-GC-MS instruments are relatively common in industrial and environmental laboratories, where they are routinely employed for contaminant analysis, and they can detect polymers down to the nanogram level. This could make them valuable as high-level NP screening tools: if polymer signals are detected at such concentrations, the sample can be considered sufficiently contaminated to warrant more targeted analyses. Though, achieving such detection limits typically requires concentrating or pre-enriching environmental samples, using techniques as those described in part I of this review. Their main limitation is the loss of particle-level information: they quantify total polymer mass but cannot resolve individual particle size, shape, or count. Nonetheless useful size-fractioned compositional data can be gathered when mass-based detection techniques are applied to sequentially filtered samples. Py-GC-MS can robustly identify polymer types and additive fingerprints, providing reliable bulk quantification, whereas MALDI-TOF offers sensitive polymer fingerprints but remains difficult to standardise because polymers ionise with different efficiencies, introducing compositional bias. As inherently destructive techniques—particularly Py-GC-MS—they are best positioned at the end of a multimodal workflow, once non-destructive, particle-based characterisation has been completed. Ultimately, their main contribution may lie in confirming polymer composition and mass balance, complementing optical methods that provide spatial and morphological detail.

3 Discussion

Alongside improvements in NPs isolation methods – discussed in part I of this review – advancing detection techniques using sophisticated analytical methods is crucial. The type of information that can be gathered through NPs characterisation includes chemical composition, particle count, size distribution, shape, surface characteristics, as well as information about sorbed organic and inorganic contaminants.

Based on the above evaluation of detection techniques, it is clear that while several existing analytical approaches can provide valuable information on NPs, no single instrument is sufficient to deliver a complete picture of their identity, morphology, and concentration across environmental matrices. To assist comparison across techniques, Table 1 summarises their practical operating windows. For each method we report whether analysis is resolved at the single NP level, what information it provides (identity, size, count, mass), conservative detection limits or ranges, sample and matrix compatibility, and typical throughput. We also flag common interferences and QA considerations. This synthesis highlights where techniques are complementary rather than redundant. For instance, coupling a particle-counting approach such as NTA or flow cytometry with a spectroscopic method (*e.g.* Raman/SERS or μFTIR) provides both quantitative and polymer-specific information. Where resources are limited or only a screening-level analysis is required, an accessible workflow could involve fluorescence-based staining and DLS/NTA to flag samples above a given particle concentration. If thresholds are exceeded, more advanced analyses such as SERS, AFM-IR, or pyrolysis-GC-MS can then be applied to confirm polymer identity, shape, and mass. Such tiered multimodal workflows balances throughput, cost, and information depth, and represents a practical strategy for developing harmonised monitoring protocols.

Table 1 Practical operating windows for nanoplastic (NP) detection methods

	Technique	NP - resolved?	Information provided						Practical range / LOD	Sample / matrix type	Throughput	Limitations/QA	Examples
			size	shape	number	Polymer ID	mass	other					
Spectroscopy	ATR-FTIR,	N*	N	N	N	Y	N		10 μm/ films ~1 μm	Dry solids, filters, extracts	High	Diffraction limited; organics overlap, water interference/rely on spectral libraries	[18, 19]
	μFTIR/FPA imaging	N*	Y	Y	N	Y	N	-	10 μm		Medium		
	LDIR	N*	Y	Y	N	Y	N	-	10 μm		High		
	LAATR-FTIR	N*	Y	Y	N	Y	N		1.3 μm	Flat solids	Low	Optical contact	[20]
	Raman micro-spectroscopy	Y	Y	Y	N	Y	N		routine ~1 μm	Solids, filters	Low	Fluorescence interference, weak signals/ Fluorescence suppression, LOD reporting	[31]
	SERS	Y	Y	Y	N	Y	N		30 nm; LOD ~0.03 μg/mL	Solids, filters suspensions	Medium	Substrate variability, fouling, blanks needed/ Spike-recovery, replicate blanks	[23, 24]
	TERS	Y	Y	Y	N	Y	N		10 nm	Solids, filters	Very low	Needs AFM tip+Raman; costly/ Proof-of-concept only	No report yet
	CARS/SRS microscopy	Y	Y	Y	N	Y	N		350 nm	Biological thin sections	Low-Med	Complex, expensive/ Bio uptake, not routine enviro	[46, 47]
	Nano-IR (AFM-IR)	Y	Y	Y	N	Y	N		50 nm	Flat Solids	Very low	Specialised instrumentation	[8]
imaging	AFM	Y	Y	Y	N	N	N	modulus	2 nm	Flat Solids	Very low	Slow, non-representative	[22]
	SEM	Y	Y	Y	N	N	N		<10 nm	Dry solids	Low	Charging, low contrast, vacuum operation/ Correlative Raman/EDX option	[20, 55]
	TEM	Y	Y	Y	N	N	N		<1 nm	Thin sections	Very low	Low contrast, artefacts, vacuum operation/ Validation, not quantification	[20, 56]
	Fluorescence microscopy	Y	Y	Y	N	N	N		~100 nm	Suspensions, sludge	Medium	Non-specific staining, autofluorescence/ Use orthogonal ID	[57]
Population analysis	DLS	N	Y	N	N	N	N	charge	1 nm–1 μm; ≥0.01–0.1 g/L	Clear suspensions	High	Polydispersity, colloids/ Refractive Index correction	[62, 63]
	NTA	N	Y	N	Y	N	N		30 nm; $\geq 10^6$–10^7/mL	Liquids	Medium	Tracking overlap, scatter/ PS standards; report lower limit	[66-68]
	Flow cytometry	Y	Y	N	Y	N	N		30 nm	Liquids	High	Non-specific staining, scatter limit/ Standardise gating, dye controls	[72]
Mass-based quantification	Py-GC/MS	N	N	N	N	Y	Y		LOD ~0.1–1 μg; LOQ ~1–10 μg	Solids, filters, tissues	Medium	Matrix organics, overlapping pyrolysates / Internal standards, mass balance	[54]
	TGA	N	N	N	N	Y	Y	kinetic	μg–mg	Solids, filters	High	Additives confound/ Bulk confirmation only	[79, 80]
	MALDI-TOF MS	N	N	N	N	Y	Y		25 ng; >200 nm	Extracted solids	Low	Ionisation bias, poor aged plastic sensitivity/ Complementary fingerprint	[82, 83]

Published on 30 2025. Downloaded on 25.5.2026 16:41:33.

Reflecting on the progress of microplastics research, a few directions for the nanoplastic field come to mind both opportunities to fast-track progress by building on lessons learned, and pitfalls to avoid. The MP community now benefit from a international standards that guide not only academic researchers but also government and industry. These standards cover statistically sound sampling protocols for environmental specimens, procedures to minimise contamination during processing, appropriate techniques and instruments for quantification and identification (*e.g.* stereomicroscopy, Raman and IR spectroscopy, Py-GC-MS), and agreed reporting norms including units, accuracy, and repeatability. The NPs field would likewise benefit from such globally standardised—or at least widely accepted—workflows if data are to be comparable across laboratories and useful for regulators and decision-makers. Much work is still needed to reach that point, and the following roadmap outlines some of the key steps that could get us there. First, promising detection techniques need to be optimised in parallel with the development of realistic reference materials that reflect the diversity of environmental NPs. Second, these materials should then be used to establish robust calibration curves and comprehensive spectral libraries, providing the foundation for reproducible and comparable analyses. Third, only then can these validated approaches be applied to tackle the unresolved challenges of environmental complexity, such as interferences from co-existing natural colloids, aggregation, and low particle concentrations, to name a few. Finally, large-scale interlaboratory and intercontinental studies will be required to test and consolidate harmonised workflows, ensuring that the community can move toward global comparability and standards.

Step 1: optimising techniques. In our view, improvements should prioritise throughput and reproducibility in already promising techniques, rather than chasing prohibitively expensive frontier instruments that remain out of reach for most laboratories. For example automated Raman systems could be improved by expanding spectral libraries and optimizing measurement parameter (wavelength, power, exposure time, spectral resolution, integration time, spectral range, accumulation, objective lens, and temperature control). Using machine learning or AI tools to automate the parameter optimisation routine over a large variety of samples could fast track the development of analytical software packages. This also holds for other spectroscopic (FTIR, XPS) and spectrometric (py-GC-MS, MALDI-ToF) techniques. Indeed, using advanced data analytics and machine learning algorithms to identify patterns and anomalies and process large data sets can further enhance the accuracy and scalability of these techniques, leading to

 This journal is © The Royal Society of Chemistry 2025

Published on 30 2025. Downloaded on 25.5.2026 16:41:33.

more reliable and effective environmental monitoring. EM and AFM-based techniques used for morphology, which are currently low throughput, would also benefit from innovations in automation. Recent advances on this front in flow cytometry are a step in the right direction,[84] with some manufacturer developing instrument specifically made to analyse sub-micron vesicles and particles.

Step 2: Concurrent step 1: standards and QA. Another important challenge in NPs analysis is controlling the quality of the data. At present, there is the lack of standardized validation protocols, insufficient diversity in reference materials, and unclear implementation of quality assurance (QA) and quality control (QC) measures, including the use of blanks and accurate identification of false positives and negatives. Model NP reference materials are needed for calibration and QC. These should mimic environmental reality by covering multiple shapes, sizes, weathering states, and additive contents. Following the lead of MP standards, these materials would underpin harmonisation and serve as benchmarks for interlaboratory studies. As for MPs, standardized validation methods should, from the onset, require performing procedures in environments with minimal plastic contamination, such as using ceramic and glass equipment and cotton lab coats ideally in a laminar flow cabinet to control airborne contaminants. Ultimately, only with appropriate reference materials can the accuracy of detection techniques be properly evaluated.

Step 3: tackling environmental complexity. Once optimised techniques and reference materials are in place, they can be applied to real samples where unresolved challenges remain. To date, most validation relies on pristine PS in simple media, but natural colloids such as clays, silica, humics, and proteins overlap with NPs in size, charge, and spectral features, producing misidentifications and false positives. Homo- and hetero-aggregation further bias distributions towards larger, easier-to-detect particles, reducing ecological representativity. Standardisation and method development must therefore explicitly account for these interferences to evaluate the accuracy of detection techniques. Using realistic standards and spectral/calibration libraries will allow methods to be stress-tested under environmental conditions, and identify which workflows are most robust to matrix effects.

Step 4: cross-laboratory studies. The final stage is validation through interlaboratory and intercontinental comparisons, akin to those already common in the MP field. Open-access databases and collaborative platforms will be essential for maintaining current QA/QC practices and providing community resources. Such efforts are critical not only for harmonising detection but also for supporting global monitoring programmes—allowing NP levels to be compared across regions, and enabling assessment of remediation strategies. Ultimately, these steps will determine whether NP research can deliver reproducible, policy-relevant datasets.

4 Conclusion

To sum up, present research does not adequately address the substantial challenges posed by the existing methods of NP detection and quantification. When it comes to accurately assessing NPs in different environments, many of these methods have limitations due to their sensitivity and specificity. In order to better monitor and analyse NPs, it is crucial to refine and develop innovative methods that can improve detection capabilities. We can better understand and reduce the risks of NPs pollution if we can close the gap between theoretical understanding and its practical application. Developing reliable detection methods is an important part of keeping the public and the environment safe as this field of study continues.

Declarations

The authors declare that they have no known competing financial interests or personal relationships that could have appeared to influence the work reported in this paper.

Author contributions

MK contributed to writing – original draft and writing – review & editing, MM contributed to writing – review & editing, and provided financial support and supervision, SCL, SJF-M and CTG contributed to writing – review and editing. All authors read and approved the final manuscript.

Conflicts of interest

The authors declare they have no competing interests.

Data availability

No primary research results, software or code have been included and no new data were generated or analysed as part of this review.

Acknowledgements

The authors wish to thank Flinders University, South Australia where this work was conducted and the Australian Research Council (ARC) for funding (FT200100301). The authors also wish to acknowledge the technical expertise of Flinders Microscopy and Microanalysis (FMMA) which is a Microscopy Australia and ANFF supported facility.

References

1 N. P. Ivleva, Chemical Analysis of Microplastics and Nanoplastics: Challenges, Advanced Methods, and Perspectives, *Chem. Rev.*, 2021, **121**(19), 11886–11936, DOI: 10.1021/acs.chemrev.1c00178.

2 I. Ali, Q. Cheng, T. Ding, Q. Yiguang, Z. Yuechao, H. Sun, C. Peng, I. Naz, J. Li and J. Liu, Micro- and nanoplastics in the environment: Occurrence, detection, characterization and

Published on 30 2025. Downloaded on 25.5.2026 16:41:33.

toxicity – A critical review, *J. Cleaner Prod.*, 2021, **313**, 127863, DOI: 10.1016/j.jclepro.2021.127863.
3 R. Thakur, V. Joshi, G. C. Sahoo, N. Jindal, R. R. Tiwari and S. Rana, Review of mechanisms and impacts of nanoplastic toxicity in aquatic organisms and potential impacts on human health, *Toxicol. Rep.*, 2025, **14**, 102013, DOI: 10.1016/j.toxrep.2025.102013.
4 S. M. Arif, I. Khan, M. Saeed, S. K. Chaudhari, M. Ghorbanpour, M. Hasan and G. Mustafa, Exploring omics solutions to reduce micro/nanoplastic toxicity in plants: A comprehensive overview, *Sci. Total Environ.*, 2025, **974**, 179220, DOI: 10.1016/j.scitotenv.2025.179220.
5 ISO, *ISO- International Organization for Standardization*, 2024, https://www.iso.org/standards.html (accessed).
6 International, A, *Helping our world work better*, 2024, https://www.astm.org/products-services/standards-and-publications.html (accessed 2024 17-11-2024).
7 D. Kalaronis, N. M. Ainali, E. Evgenidou, G. Z. Kyzas, X. Yang, D. N. Bikiaris and D. A. Lambropoulou, Microscopic techniques as means for the determination of microplastics and nanoplastics in the aquatic environment: A concise review, *Green Anal. Chem.*, 2022, **3**, 100036, DOI: 10.1016/j.greeac.2022.100036.
8 C. Prater, K. Kjoller and R. Shetty, Nanoscale infrared spectroscopy, *Mater. Today*, 2010, **13**(11), 56–60, DOI: 10.1016/S1369-7021(10)70205-4.
9 S. Mariano, S. Tacconi, M. Fidaleo, M. Rossi and L. Dini, Micro and Nanoplastics Identification: Classic Methods and Innovative Detection Techniques, *Front. Toxicol.*, 2021, **3**, 636640, DOI: 10.3389/ftox.2021.636640, From NLM.
10 S. Morgana, B. Casentini, V. Tirelli, F. Grasso and S. Amalfitano, Fluorescence-based detection: A review of current and emerging techniques to unveil micro/nanoplastics in environmental samples, *TrAC, Trends Anal. Chem.*, 2024, **172**, 117559, DOI: 10.1016/j.trac.2024.117559.
11 H. Cai, F. Du, J. Gigault and H. Shi, in *Analysis of Microplastics and Nanoplastics*, ed. H. Shi and C. Sun, Elsevier, 2025, ch. 20 – The challenges and perspectives of nanoplastic analysis, pp. 379–395.
12 J. Xie, A. Gowen, W. Xu and J. Xu, Analysing micro- and nanoplastics with cutting-edge infrared spectroscopy techniques: a critical review, *Anal. Methods*, 2024, **16**(15), 2177–2197, DOI: 10.1039/D3AY01808C.
13 A. Nene, S. Sadeghzade, S. Viaroli, W. Yang, U. P. Uchenna, A. Kandwal, X. Liu, P. Somani and M. Galluzzi, Recent advances and future technologies in nano-microplastics detection, *Environ. Sci. Eur.*, 2025, **37**(1), 7, DOI: 10.1186/s12302-024-01044-y.
14 S. J. Fraser-Miller, J. Saarinen and C. J. Strachan, Vibrational Spectroscopic Imaging, in *Analytical Techniques in the Pharmaceutical Sciences*, ed. A. Müllertz, Y. Perrie and T. Rades, Springer New York, 2016, pp. 523–589.
15 P. J. Larkin, *Infrared and Raman spectroscopy : principles and spectral interpretation*, Elsevier, 2018.
16 G. Liu, Z. Zhu, Y. Yang, Y. Sun, F. Yu and J. Ma, Sorption behavior and mechanism of hydrophilic organic chemicals to virgin and aged microplastics in freshwater and seawater, *Environ. Pollut.*, 2019, **246**, 26–33, DOI: 10.1016/j.envpol.2018.11.100.
17 F. Corami, B. Rosso, B. Bravo, A. Gambaro and C. Barbante, A novel method for purification, quantitative analysis and characterization of microplastic fibers using Micro-FTIR, *Chemosphere*, 2020, **238**, 124564, DOI: 10.1016/j.chemosphere.2019.124564.
18 Y. Liu, S. Lüttjohann, A. Vianello, C. Lorenz, F. Liu and J. Vollertsen, Detecting small microplastics down to 1.3 μm using large area ATR-FTIR, *Mar. Pollut. Bull.*, 2024, **198**, 115795, DOI: 10.1016/j.marpolbul.2023.115795.
19 L. M. Hernandez, E. G. Xu, H. C. E. Larsson, R. Tahara, V. B. Maisuria and N. Tufenkji, Plastic Teabags Release Billions of Microparticles and Nanoparticles into Tea, *Environ. Sci. Technol.*, 2019, **53**(21), 12300–12310, DOI: 10.1021/acs.est.9b02540.
20 C. Schwaferts, R. Niessner, M. Elsner and N. P. Ivleva, Methods for the analysis of submicrometer- and nanoplastic particles in the environment, *TrAC, Trends Anal. Chem.*, 2019, **112**, 52–65, DOI: 10.1016/j.trac.2018.12.014.
21 S. Xu, C. Wang, P. Zhu, D. Zhang and X. Pan, Temporospatial nano-heterogeneity of self-assembly of extracellular polymeric substances on microplastics and water environmental implications, *J. Hazard. Mater.*, 2022, **440**, 129773, DOI: 10.1016/j.jhazmat.2022.129773.
22 D. Xie, H. Fang, X. Zhao, Y. Lin and Z. Su, Identification of microplastics and nanoplastics in environmental water by AFM-IR, *Anal. Chim. Acta*, 2025, **1354**, 343992, DOI: 10.1016/j.aca.2025.343992.
23 F. Xing, W. Duan, J. Tang, Y. Zhou, Z. Guo, H. Zhang, J. Xiong and M. Fan, Superhydrophobic Surface-Enhanced Raman Spectroscopy (SERS) Substrates for Sensitive Detection of Trace Nanoplastics in Water, *Anal. Chem.*, 2025, **97**(4), 2293–2299, DOI: 10.1021/acs.analchem.4c05554.
24 Z. Yang, K. Zhu, K. Yang, Y. Qing, Y. Zhao, L. Wu, S. Zong, Y. Cui and Z. Wang, One-step detection of nanoplastics in aquatic environments using a portable SERS chessboard substrate, *Talanta*, 2025, **282**, 127076, DOI: 10.1016/j.talanta.2024.127076.
25 Z. Dai, Q. Zhang, Y. Zhao, Y. Li, Y. Huang, Z. Li, F. Wei and F. Shao, Nanospectroscopic Imaging of 2D Materials by Tip-Enhanced Raman Spectroscopy, *J. Phys. Chem. C*, 2025, **129**(16), 7591–7611, DOI: 10.1021/acs.jpcc.5c01637.
26 D. Mrđenović, D. Abbott, V. Mougel, W. Su, N. Kumar and R. Zenobi, Visualizing Surface Phase Separation in PS-PMMA Polymer Blends at the Nanoscale, *ACS Appl. Mater. Interfaces*, 2022, **14**(21), 24938–24945, DOI: 10.1021/acsami.2c03857.
27 T. Takahashi, K. P. Herdzik, K. N. Bourdakos, J. A. Read and S. Mahajan, Selective Imaging of Microplastic and Organic Particles in Flow by Multimodal Coherent Anti-Stokes Raman Scattering and Two-Photon Excited Autofluorescence Analysis, *Anal. Chem.*, 2021, **93**(12), 5234–5240, DOI: 10.1021/acs.analchem.0c05474.
28 S. Adhikari, V. Kelkar, R. Kumar and R. U. Halden, Methods and challenges in the detection of microplastics and

 This journal is © The Royal Society of Chemistry 2025

Published on 30 2025. Downloaded on 25.5.2026 16:41:33.

nanoplastics: a mini-review, *Polym. Int.*, 2022, **71**(5), 543–551, DOI: 10.1002/pi.6348.

29 In *Infrared and Raman Spectroscopy*, ed. P. J. Larkin, Elsevier, 2nd edn, 2018, p. iii.

30 C. Fang, Z. Sobhani, X. Zhang, L. McCourt, B. Routley, C. T. Gibson and R. Naidu, Identification and visualisation of microplastics / nanoplastics by Raman imaging (iii): algorithm to cross-check multi-images, *Water Res.*, 2021, **194**, 116913, DOI: 10.1016/j.watres.2021.116913.

31 Z. Sobhani, X. Zhang, C. Gibson, R. Naidu, M. Mallavarapu and C. Fang, Identification and visualisation of microplastics/nanoplastics by Raman imaging (i): Down to 100 nm, *Water Res.*, 2020, **174**, 115658, DOI: 10.1016/j.watres.2020.115658.

32 C. Schwaferts, V. Sogne, R. Welz, F. Meier, T. Klein, R. Niessner, M. Elsner and N. P. Ivleva, Nanoplastic Analysis by Online Coupling of Raman Microscopy and Field-Flow Fractionation Enabled by Optical Tweezers, *Anal. Chem.*, 2020, **92**(8), 5813–5820, DOI: 10.1021/acs.analchem.9b05336.

33 X.-X. Zhou, R. Liu, L.-T. Hao and J.-F. Liu, Identification of polystyrene nanoplastics using surface enhanced Raman spectroscopy, *Talanta*, 2021, **221**, 121552, DOI: 10.1016/j.talanta.2020.121552.

34 F. Adar, *Depth Resolution of the Raman Microscope: Optical Limitations and Sample Characteristics*, 2010, https://www.spectroscopyonline.com/view/depth-resolution-raman-microscope-optical-limitations-and-sample-characteristics (accessed).

35 K. Samir, K. Prabhat, D. Anamika and P. Chandra Shakher, Surface-Enhanced Raman Scattering: Introduction and Applications, in *Recent Advances in Nanophotonics*, ed. K. Mojtaba and A. S. Parsoua, IntechOpen, 2020, ch. 8.

36 R. Hu, K. Zhang, W. Wang, L. Wei and Y. Lai, Quantitative and sensitive analysis of polystyrene nanoplastics down to 50 nm by surface-enhanced Raman spectroscopy in water, *J. Hazard. Mater.*, 2022, **429**, 128388, DOI: 10.1016/j.jhazmat.2022.128388.

37 L. Lv, L. He, S. Jiang, J. Chen, C. Zhou, J. Qu, Y. Lu, P. Hong, S. Sun and C. Li, In situ surface-enhanced Raman spectroscopy for detecting microplastics and nanoplastics in aquatic environments, *Sci. Total Environ.*, 2020, **728**, 138449, DOI: 10.1016/j.scitotenv.2020.138449.

38 P. Zhang, Y. Wang, X. Zhao, Y. Ji, R. Mei, L. Fu, M. Man, J. Ma, X. Wang and L. Chen, Surface-enhanced Raman scattering labeled nanoplastic models for reliable bio-nano interaction investigations, *J. Hazard. Mater.*, 2022, **425**, 127959, DOI: 10.1016/j.jhazmat.2021.127959, From NLM.

39 D. Kurouski, A. Dazzi, R. Zenobi and A. Centrone, Infrared and Raman chemical imaging and spectroscopy at the nanoscale, *Chem. Soc. Rev.*, 2020, **49**(11), 3315–3347, DOI: 10.1039/C8CS00916C.

40 C. Chen, N. Hayazawa and S. Kawata, A 1.7 nm resolution chemical analysis of carbon nanotubes by tip-enhanced Raman imaging in the ambient, *Nat. Commun.*, 2014, **5**(1), 3312, DOI: 10.1038/ncomms4312.

41 B.-S. Yeo, E. Amstad, T. Schmid, J. Stadler and R. Zenobi, Nanoscale Probing of a Polymer-Blend Thin Film with Tip-Enhanced Raman Spectroscopy, *Small*, 2009, **5**(8), 952–960, DOI: 10.1002/smll.200801101.

42 J. Piwowarczyk, R. Jędrzejewski, D. Moszyński, K. Kwiatkowski, A. Niemczyk and J. Baranowska, XPS and FTIR Studies of Polytetrafluoroethylene Thin Films Obtained by Physical Methods, *Polymers*, 2019, **11**(10), 1629, DOI: 10.3390/polym11101629.

43 S. Lu, K. Zhu, W. Song, G. Song, D. Chen, T. Hayat, N. S. Alharbi, C. Chen and Y. Sun, Impact of water chemistry on surface charge and aggregation of polystyrene microspheres suspensions, *Sci. Total Environ.*, 2018, **630**, 951–959, DOI: 10.1016/j.scitotenv.2018.02.296.

44 X. Xi, L. Wang, T. Zhou, J. Yin, H. Sun, X. Yin and N. Wang, Effects of physicochemical factors on the transport of aged polystyrene nanoparticles in saturated porous media, *Chemosphere*, 2022, **289**, 133239, DOI: 10.1016/j.chemosphere.2021.133239.

45 G. H. Major, J. W. Pinder, D. E. Austin, D. R. Baer, S. L. Castle, J. Čechal, B. M. Clark, H. Cohen, J. Counsell and A. Herrera-Gomez, *et al.*, Perspective on improving the quality of surface and material data analysis in the scientific literature with a focus on x-ray photoelectron spectroscopy (XPS), *J. Vac. Sci. Technol., A*, 2023, **41**(3), 038501, DOI: 10.1116/6.0002437, (acccessed 6/13/2023).

46 N. Qian, X. Gao, X. Lang, H. Deng, T. M. Bratu, Q. Chen, P. Stapleton, B. Yan and W. Min, Rapid single-particle chemical imaging of nanoplastics by SRS microscopy, *Proc. Natl. Acad. Sci. U. S. A.*, 2024, **121**(3), e2300582121, DOI: 10.1073/pnas.2300582121.

47 J. Ao, G. Xu, H. Wu, L. Xie, J. Liu, K. Gong, X. Ruan, J. Han, K. Li and W. Wang, *et al.*, Fast detection and 3D imaging of nanoplastics and microplastics by stimulated Raman scattering microscopy, *Cell Rep. Phys. Sci.*, 2023, **4**(10), 101623, DOI: 10.1016/j.xcrp.2023.101623.

48 B. Nguyen and N. Tufenkji, Single-Particle Resolution Fluorescence Microscopy of Nanoplastics, *Environ. Sci. Technol.*, 2022, **56**(10), 6426–6435, DOI: 10.1021/acs.est.1c08480.

49 C. Fang, Y. Luo and R. Naidu, Advancements in Raman imaging for nanoplastic analysis: Challenges, algorithms and future Perspectives, *Anal. Chim. Acta*, 2024, **1290**, 342069, DOI: 10.1016/j.aca.2023.342069.

50 Eurofins, *Atomic Force Microscopy (AFM)*, 2025, https://www.eag.com/techniques/imaging/atomic-force-microscopy-afm/ (accessed 2025).

51 N. Ishida, in *Non-Destructive Material Characterization Methods*, ed. A. Otsuki, S. Jose, M. Mohan and S. Thomas, Elsevier, 2024, ch. 4 – Atomic force microscopy, pp. 89–125.

52 M. Galluzzi, M. Lancia, C. Zheng, V. Re, V. Castelvetro, S. Guo and S. Viaroli, Atomic Force Microscopy (AFM) nanomechanical characterization of micro- and nanoplastics to support environmental investigations in groundwater, *Emerging Contam.*, 2025, **11**(2), 100478, DOI: 10.1016/j.emcon.2025.100478.

Published on 30 2025. Downloaded on 25.5.2026 16:41:33.

53 V. Budhiraja, P. M. Shandilya, L. Pavko, J. I. Garver and A. Kržan, Influence of aging and colorants on environmental degradation of polyolefins, *Emerging Contam.*, 2025, **11**(3), 100516, DOI: 10.1016/j.emcon.2025.100516.
54 X.-X. Zhou, S. He, Y. Gao, H.-Y. Chi, D.-J. Wang, Z.-C. Li and B. Yan, Quantitative Analysis of Polystyrene and Poly(methyl methacrylate) Nanoplastics in Tissues of Aquatic Animals, *Environ. Sci. Technol.*, 2021, **55**(5), 3032–3040, DOI: 10.1021/acs.est.0c08374.
55 Y. Wang, Z. Wang, X. Lu, H. Zhang and Z. Jia, Simulation and Characterization of Nanoplastic Dissolution under Different Food Consumption Scenarios, *Toxics*, 2023, **11**(7), 550.
56 X. Li, E. He, B. Xia, C. A. M. Van Gestel, W. J. G. M. Peijnenburg, X. Cao and H. Qiu, Impact of CeO2 nanoparticles on the aggregation kinetics and stability of polystyrene nanoplastics: Importance of surface functionalization and solution chemistry, *Water Res.*, 2020, **186**, 116324, DOI: 10.1016/j.watres.2020.116324.
57 L. Zhang, G. Li, Q. Xin, H. Liu, X. Yang and Y. Liu, AIE-labeled fluorescent polystyrene nanoplastics for quantitative analysis in macrophages uptake, *Sens. Actuators, B*, 2024, **413**, 135878, DOI: 10.1016/j.snb.2024.135878.
58 Z. Wang, N. K. Saadé and P. A. Ariya, Advances in Ultra-Trace Analytical Capability for Micro/Nanoplastics and Water-Soluble Polymers in the Environment: Fresh Falling Urban Snow, *Environ. Pollut.*, 2021, **276**, 116698, DOI: 10.1016/j.envpol.2021.116698.
59 Y. Liu, Y. Wang, N. Li and S. Jiang, Avobenzone and nanoplastics affect the development of zebrafish nervous system and retinal system and inhibit their locomotor behavior, *Sci. Total Environ.*, 2022, **806**, 150681, DOI: 10.1016/j.scitotenv.2021.150681.
60 V. Martinez and M. Henary, Nile Red and Nile Blue: Applications and Syntheses of Structural Analogues, *Chem. – Eur. J.*, 2016, **22**(39), 13764–13782, DOI: 10.1002/chem.201601570.
61 B. J. Frisken, Revisiting the method of cumulants for the analysis of dynamic light-scattering data, *Appl. Opt.*, 2001, **40**(24), 4087–4091, DOI: 10.1364/AO.40.004087.
62 R. Biba, P. Cvjetko, M. Jakopčić, B. Komazec, M. Tkalec, N. Dimitrov, T. Begović and B. Balen, Phytotoxic Effects of Polystyrene and Polymethyl Methacrylate Microplastics on Allium cepa Roots, *Plants*, 2023, **12**(4), 747.
63 C.-S. Chen, C. Le, M.-H. Chiu and W.-C. Chin, The impact of nanoplastics on marine dissolved organic matter assembly, *Sci. Total Environ.*, 2018, **634**, 316–320, DOI: 10.1016/j.scitotenv.2018.03.269.
64 C. M. Maguire, M. Rösslein, P. Wick and A. Prina-Mello, Characterisation of particles in solution - a perspective on light scattering and comparative technologies, *Sci. Technol. Adv. Mater.*, 2018, **19**(1), 732–745, DOI: 10.1080/14686996.2018.1517587, From NLM.
65 V. Filipe, A. Hawe and W. Jiskoot, Critical evaluation of Nanoparticle Tracking Analysis (NTA) by NanoSight for the measurement of nanoparticles and protein aggregates, *Pharm. Res.*, 2010, **27**(5), 796–810, DOI: 10.1007/s11095-010-0073-2, From NLM.
66 Y.-S. Chang, S.-H. Chou, Y.-J. Jhang, T.-S. Wu, L.-X. Lin, Y.-L. Soo and I. L. Hsiao, Extraction method development for nanoplastics from oyster and fish tissues, *Sci. Total Environ.*, 2022, **814**, 152675, DOI: 10.1016/j.scitotenv.2021.152675.
67 J. Zhang, M. Peng, E. Lian, L. Xia, A. G. Asimakopoulos, S. Luo and L. Wang, Identification of Poly(ethylene terephthalate) Nanoplastics in Commercially Bottled Drinking Water Using Surface-Enhanced Raman Spectroscopy, *Environ. Sci. Technol.*, 2023, **57**(22), 8365–8372, DOI: 10.1021/acs.est.3c00842.
68 S.-H. Chou, Y.-K. Chuang, C.-M. Lee, Y.-S. Chang, Y.-J. Jhang, C.-W. Yeh, T.-S. Wu, C.-Y. Chuang and I. L. Hsiao, Visualization and (Semi-)quantification of submicrometer plastics through scanning electron microscopy and time-of-flight secondary ion mass spectrometry, *Environ. Pollut.*, 2022, **300**, 118964, DOI: 10.1016/j.envpol.2022.118964.
69 H. Mekaru, Effect of Agitation Method on the Nanosized Degradation of Polystyrene Microplastics Dispersed in Water, *ACS Omega*, 2020, **5**(7), 3218–3227, DOI: 10.1021/acsomega.9b03278.
70 K. M. McKinnon, Flow Cytometry: An Overview, *Curr. Protoc. Immunol.*, 2018, **120**, 5.1.1–5.1.11, DOI: 10.1002/cpim.40, From NLM.
71 S. Morgana, B. Casentini and S. Amalfitano, Uncovering the release of micro/nanoplastics from disposable face masks at times of COVID-19, *J. Hazard. Mater.*, 2021, **419**, 126507, DOI: 10.1016/j.jhazmat.2021.126507.
72 N. Kaile, M. Lindivat, J. Elio, G. Thuestad, Q. G. Crowley and I. A. Hoell, Preliminary Results From Detection of Microplastics in Liquid Samples Using Flow Cytometry, *Front. Mar. Sci.*, 2020, **7**, 552688, DOI: 10.3389/fmars.2020.552688.
73 W. Bauten, M. Nöth, T. Kurkina, F. Contreras, Y. Ji, C. Desmet, M.-Á. Serra, D. Gilliland and U. Schwaneberg, Plastibodies for multiplexed detection and sorting of microplastic particles in high-throughput, *Sci. Total Environ.*, 2023, **860**, 160450, DOI: 10.1016/j.scitotenv.2022.160450.
74 A. Ter Halle, L. Jeanneau, M. Martignac, E. Jardé, B. Pedrono, L. Brach and J. Gigault, Nanoplastic in the North Atlantic Subtropical Gyre, *Environ. Sci. Technol.*, 2017, **51**(23), 13689–13697, DOI: 10.1021/acs.est.7b03667.
75 A. Wahl, C. Le Juge, M. Davranche, H. El Hadri, B. Grassl, S. Reynaud and J. Gigault, Nanoplastic occurrence in a soil amended with plastic debris, *Chemosphere*, 2021, **262**, 127784, DOI: 10.1016/j.chemosphere.2020.127784.
76 D. Materić, A. Kasper-Giebl, D. Kau, M. Anten, M. Greilinger, E. Ludewig, E. van Sebille, T. Röckmann and R. Holzinger, Micro- and Nanoplastics in Alpine Snow: A New Method for Chemical Identification and (Semi)Quantification in the Nanogram Range, *Environ. Sci. Technol.*, 2020, **54**(4), 2353–2359, DOI: 10.1021/acs.est.9b07540.
77 E. D. Okoffo and K. V. Thomas, Quantitative analysis of nanoplastics in environmental and potable waters by pyrolysis-gas chromatography–mass spectrometry, *J. Hazard. Mater.*, 2024, **464**, 133013, DOI: 10.1016/j.jhazmat.2023.133013.

 This journal is © The Royal Society of Chemistry 2025

Published on 30 2025. Downloaded on 25.5.2026 16:41:33.

78 M. Majewsky, H. Bitter, E. Eiche and H. Horn, Determination of microplastic polyethylene (PE) and polypropylene (PP) in environmental samples using thermal analysis (TGA-DSC), *Sci. Total Environ.*, 2016, **568**, 507–511, DOI: 10.1016/j.scitotenv.2016.06.017.

79 E. Dümichen, P. Eisentraut, C. G. Bannick, A. K. Barthel, R. Senz and U. Braun, Fast identification of microplastics in complex environmental samples by a thermal degradation method, *Chemosphere*, 2017, **174**, 572–584, DOI: 10.1016/j.chemosphere.2017.02.010, From NLM.

80 J. Yu, P. Wang, F. Ni, J. Cizdziel, D. Wu, Q. Zhao and Y. Zhou, Characterization of microplastics in environment by thermal gravimetric analysis coupled with Fourier transform infrared spectroscopy, *Mar. Pollut. Bull.*, 2019, **145**, 153–160, DOI: 10.1016/j.marpolbul.2019.05.037.

81 W. Fu, J. Min, W. Jiang, Y. Li and W. Zhang, Separation, characterization and identification of microplastics and nanoplastics in the environment, *Sci. Total Environ.*, 2020, **721**, 137561, DOI: 10.1016/j.scitotenv.2020.137561.

82 Y. Lin, X. Huang, Q. Liu, Z. Lin and G. Jiang, Thermal fragmentation enhanced identification and quantification of polystyrene micro/nanoplastics in complex media, *Talanta*, 2020, **208**, 120478, DOI: 10.1016/j.talanta.2019.120478, From NLM.

83 P. Wu, Y. Tang, G. Cao, J. Li, S. Wang, X. Chang, M. Dang, H. Jin, C. Zheng and Z. Cai, Determination of Environmental Micro(Nano)Plastics by Matrix-Assisted Laser Desorption/Ionization–Time-of-Flight Mass Spectrometry, *Anal. Chem.*, 2020, **92**(21), 14346–14356, DOI: 10.1021/acs.analchem.0c01928.

84 Center, U. o. M. N., *University of Minnesota Nano Center Standard Operating Procedure*, 2019, https://apps.mnc.umn.edu/pub/equipment/nanoflex_sop.pdf (accessed 2024 18-09-2024).